

Recent Advances of 2D Materials in Nonlinear Photonics and Fiber Lasers

Wenjun Liu, Mengli Liu, Ximei Liu, Xiaoting Wang, Hui-Xiong Deng, Ming Lei,*
Zhongming Wei,* and Zhiyi Wei

The explosive success of graphene opens a new era of ultrathin 2D materials. It has been realized that the van der Waals layered materials with atomic and less atomic thickness can not only exist stably, but also exhibit unique and technically useful properties including small size effect, surface effect, macro quantum tunnel effect, and quantum effect. With the extensive research and revealing of the basic optical properties and new photophysical properties of 2D materials, a series of potential applications in optical devices have been continuously demonstrated and realized, which immediately roused an upsurge of study in the academic circle. Therefore, the application of 2D materials as broadband, efficient, convenient, and versatile saturable absorbers in ultrafast lasers is a potential and promising field. Herein, the main preparation methods of 2D materials are reviewed and technical guidelines for identifying and characterizing layered 2D materials are provided. After investigating the characteristics of 2D materials thoroughly in nonlinear optics, their performances in fiber lasers are comprehensively summarized according to the types of materials. Finally, some developmental challenges, potential prospects, and future research directions are summarized and presented for such promising materials.

1. Introduction

As early as 1959, Richard Feynman has mentioned the concept of layered materials in his speech entitled “There is enough space at the bottom.”^[1] However, until today, decades later, we just seem to have a clearer understanding of this mysterious species—2D materials through persistent efforts.^[2] For 2D materials with nanostructures, the unique physical singularities occur when heat transfer and charge are determined on a plane, which makes them attracted much attention from ultrafast photonics,^[3–9] electronics/optoelectronics devices,^[10–22] high-performance sensors,^[23–30] biomedicine^[31–42] to optical modulation.^[43–51] In the past few years, the overall pattern of 2D materials has not only been greatly expanded but also greatly innovated in its development and application. One of the most compelling applications is nonlinear optics, which has created a frenzy for laser innovation.

Among many available ultrashort pulse generation technologies, passively mode-locked fiber laser (MLFL) based on saturable absorber (SA) has become one of the most effective ways to achieve ultrashort pulses because of its advantages of good beam quality, compact structure, low cost, and good compatibility. Although the development of SAs has gone through dyes, semiconductor saturable absorber mirrors (SESAMs), etc., since the successful preparation and application of graphene materials, there has been an upsurge in the preparation research of SAs based on 2D materials in fiber lasers. Due to the optical nonlinearity of 2D materials, the SAs which based on 2D materials can periodically modulate the circulating light field in the laser cavity, causing a large number of longitudinal modes to phase oscillation, thus forming regular short pulse trains in the time domain. The mechanism of nonlinear absorption is mainly caused by the Pauli incompatibility principle, which enables the material to absorb less instantaneously when a large number of electrons are found in the up-excited state under the action of strong light.


Since the advent of graphene, more 2D materials have been recognized and applied in laser. Until now, the research hotspots are mainly concentrated on several representative materials or some heterojunction material about them, including 1) Graphene; 2) topological insulators (TIs); 3) black phosphorus

Dr. W. Liu, M. Liu, X. Liu, Dr. X. Wang, Prof. M. Lei
State Key Laboratory of Information Photonics
and Optical Communications
School of Science
Beijing University of Posts and Telecommunications
P.O. Box 91, Beijing 100876, China
E-mail: mlei@bupt.edu.cn

Dr. W. Liu, Prof. Z. Y. Wei
Beijing National Laboratory for Condensed Matter Physics
Institute of Physics
Chinese Academy of Sciences
Beijing 100190, China

Dr. X. Wang, Prof. H.-X. Deng, Prof. Z. Wei
State Key Laboratory of Superlattices and Microstructures
Institute of Semiconductors
Chinese Academy of Sciences & Center of Materials Science
and Optoelectronics Engineering
University of Chinese Academy of Sciences
Beijing 100083, China
E-mail: zmwei@semi.ac.cn

Prof. Z. Wei
Beijing Academy of Quantum Information Sciences
Beijing 100193, China

 The ORCID identification number(s) for the author(s) of this article can be found under <https://doi.org/10.1002/adom.201901631>.

DOI: 10.1002/adom.201901631

(BPs); 4) transition metal dichalcogenides (TMDs). Substantial research indicating that many similar photonic properties are shared in 2D materials as saturable absorbers, such as broadband absorption, strong nonlinearity, ultrafast response time, and saturable absorption characteristics.^[52–62] Sufficient researches have shown that the application of 2D materials as broadband, economical, efficient, and widely used optical modulators in ultrafast lasers is a potential and high-speed development area with broad commercial prospects.

Here, a comprehensive review to retrospect the recent progress in 2D materials and prospect for the avenues and opportunities of future work are necessary, which not only clarifies the development stage at this moment, but also provides feasible direction and guidance for future explorations. In this paper, the synthesis, characterization, and nonlinearity of 2D materials are reviewed, and their performances in fiber lasers are comprehensively summarized according to the types of materials. Finally, some of the major development challenges faced by 2D materials are discussed and a bold outlook for their future direction is made.

2. Synthesis

In recent years, various preparation methods have been successfully applied to the fabrication of 2D materials, which is roughly encompassed as top-down and bottom-up methods. Here, two common methods from each of them are selected for a detailed introduction.

In mechanical exfoliation, bulk crystals placed on the scotch tape is repeatedly pasted and peeled off to obtain thin layered sheets. Such a simple lift-off process benefits from the weak van der Waals force between layers of 2D materials. In this way, the graphene was successfully stripped from the graphite flakes by Geim and Novoselov for the first time.^[63] This method has advantages of convenience in operation and low cost, and the products maintain high crystallinity and structural integrity. However, because of the inefficiency and uncontrollability of manual operation, the yield of the obtained material is small and the number of layers is random.^[64–66]

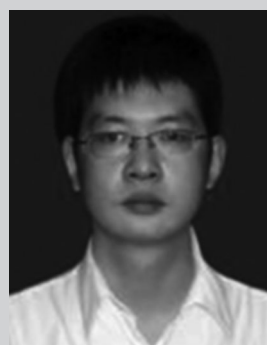
High-yield liquid exfoliation as an efficient alternative to mechanical exfoliation has been increasingly used.^[67–74] There are two ideas for how to destroy interlayer forces. One is to widen the interlayer distance by embedding organic or ionic materials, which leads to the weakening of the interlayer adhesion force. The other is to directly use high-intensity ultrasonic to produce microbubbles and forces in materials. These two are the main operational principle of lithium-ion intercalation exfoliation and liquid-phase exfoliation. In lithium-ion intercalation exfoliation, the intercalation of lithium ions combining with mechanical forces such as stirring or ultrasonication tends to produce high-yield few-layer materials. However, this method may alter the structure of the material, and the quality needs to be further improved.

In pulsed laser deposition (PLD) technology,^[50,75] the high-energy pulses strike the solid target, and the material is separated from the target to form a plasma plume, after which the molten material transfer to the substrate surface, film nucleation and formation were finally formed on the surface of the substrate. The deposition rate of this preparation method is high and the prepared film is uniform. However, the quality of



Wenjun Liu received his Ph.D. degree from Beijing University of Posts and Telecommunications, Beijing, China, in 2011. Then, he was a postdoctoral fellow in the Laboratory of Optical Physics, Institute of Physics, Chinese Academy of Sciences from 2012 to 2015. He is currently a professor at Beijing University of Posts and

Telecommunications. His research interests include ultrafast and ultrahigh intensity laser technology, and advanced material for ultrafast photonics.



Ming Lei received his Ph.D. from Institute of Physics, Chinese Academy of Science in 2007. He worked as a postdoctoral fellow at the Hong Kong University of Science and Technology and Chinese University of Hong Kong from 2007 to 2008 and from 2009 to 2010, respectively. He is now a professor in Beijing University of Posts

and Telecommunications. His research group focuses on synthesis of low-dimensional semiconductor and related photoelectric properties.



Zhongming Wei received his B.S. from Wuhan University (China) in 2005, and Ph.D. from Institute of Chemistry, Chinese Academy of Sciences in 2010 under the supervision of Prof. Daoben Zhu and Prof. Wei Xu. From 2010 to 2015, he worked as a postdoctoral fellow and then became an assistant professor in Prof. Thomas

Bjørnholm's group at University of Copenhagen, Denmark. Currently, he is working as a professor at Institute of Semiconductors, Chinese Academy of Sciences. His research interests include low-dimensional semiconductors and their (opto)electronic devices.

the film needs to be improved, and it is unable to achieve large-area laser deposition under existing technology

Chemical vapor deposition (CVD) is a process in which gaseous or vapor-state chemicals are chemically reacted to form solid sediments on the surface of the substrate in the reactor by heating.^[76] CVD method has been widely used in many fields because of the superiorities in density, high crystallinity, and uniformity. Moreover, it is able to realize mass production.^[49]

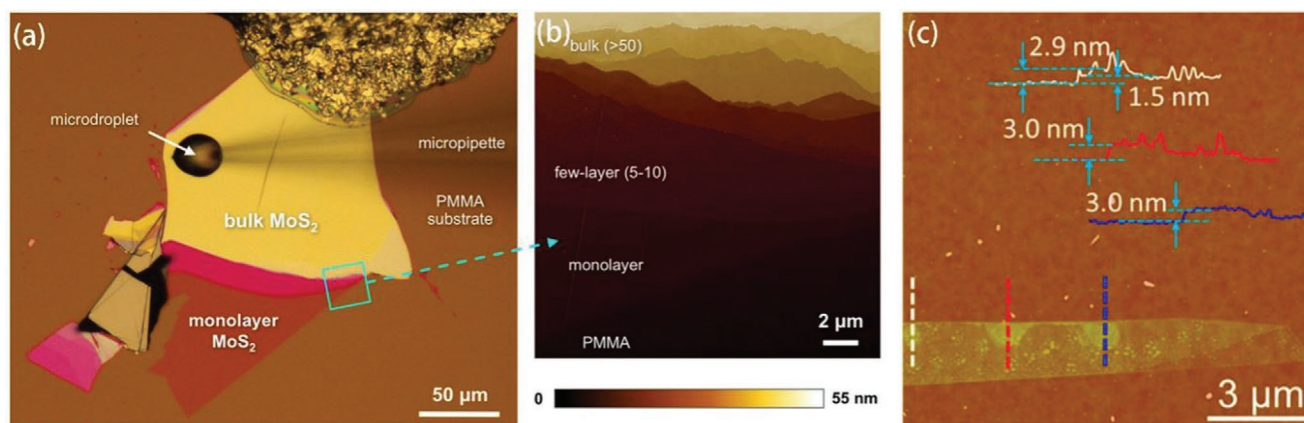


Figure 1. a) Optical micrograph of a MoS₂ flake. b) AFM of selected green rectangular area in (a). Reproduced with permission.^[81] Copyright 2016, American Chemical Society. c) Height information at different locations in AFM. Reproduced with permission.^[82] Copyright 2014, American Chemical Society.

However, this method has high cost and complexity, and it is often accompanied by the follow-up process of film transfer.

3. Characterization

3.1. Atomic Force Microscopy

Atomic force microscope (AFM) is an important technique for obtaining surface information of materials. It performs excellently in applications due to 3D surface images and high resolution.^[77–80] The emergence of AFM has undoubtedly promoted the development of nanotechnology. It is able to provide surface information for samples with various types, and observe the surface of the sample at high magnification under atmospheric conditions (Figure 1).^[81,82] Wide range of applications, strong software processing capabilities, high resolution, and nondestructive to samples make it outstanding in applications. However, the acquisition of high precision is bound to be at the expense of imaging range and scanning speed, and the requirements for the probe are high during measurement.

3.2. Transmission Electron Microscopy

Transmission electron microscopy (TEM) is an effective tool for observing and analyzing the morphology, organization, and structure of materials, in which electron beams are used as illumination sources to analyze the microstructure of the samples through the images formed by transmission electron beams or diffraction electron beams.^[83,84] Two imaging modes are included in TEM, one is microscopic imaging (Figure 2a) for tissue morphology observation, the other is diffraction imaging for isotope analysis of crystal structures (illustration in Figure 2a).^[83] In scanning transmission electron microscopy (STEM), the large angle annular dark field detectors combined with electron energy loss spectroscopy make individual atoms visible. The STEM image of MoS₂ given by George et al. clearly shows the structure of the material (Figure 2b).^[85] Li et al. also accurately locates the growth edges of WSe₂ and MoS₂ in the prepared heterojunctions (Figure 2c).^[86]

3.3. X-Ray Diffraction

X-ray diffraction (XRD), as a nondestructive analysis method for the characterization of crystal phase and structure, has become one of the most basic and important structural testing methods. When the sample is irradiated by strong X-rays, the identifying X-rays are excited from the sample. The characteristics of elements and the distribution of atoms in crystals can be judged by the diffraction peaks of rays and the corresponding intensity information.^[87] XRD can also be used to roughly determine the number of layers of nanosheets. For example, bulk MoS₂ often tends to show all three reflection modes (100), (110), and (002), but in single-layer MoS₂, the reflection peak (002) is missing (Figure 3).^[83,88]

3.4. X-Ray Photoelectron Spectroscopy

X-ray photoelectron spectroscopy (XPS) can not only reflect the molecular structure of a substance through the valence state of a molecule, but also provide information on the component content and chemical bond of a compound for electronic material research.^[89,90] Su et al. qualitatively and quantitatively monitored the ratio of Mo–Se and (Mo–Se + Mo–S) during the selenization process of MoS₂.^[91] When the temperature reaches up to 900 °C, only the characteristic XPS peaks of WSe₂ are observed. Besides, XPS can also be used as a method to distinguish and identify the crystal phase of 2D materials. Because of the inevitable inherent shortcomings of lithium-ion intercalation, phase transformation may occur in the materials prepared by this method. Chhowalla and co-workers reported this phenomenon. They not only identified the different phases, but also further quantitatively calculated the concentrations of the various phases by XPS (Figure 4).^[92]

3.5. Raman Spectroscopy

Generally speaking, Raman spectroscopy is recognized as a unique chemical fingerprint of specific material or molecule, therefore can be used to effectively distinguish different substances or to accurately identify the constituents of substances.^[93]

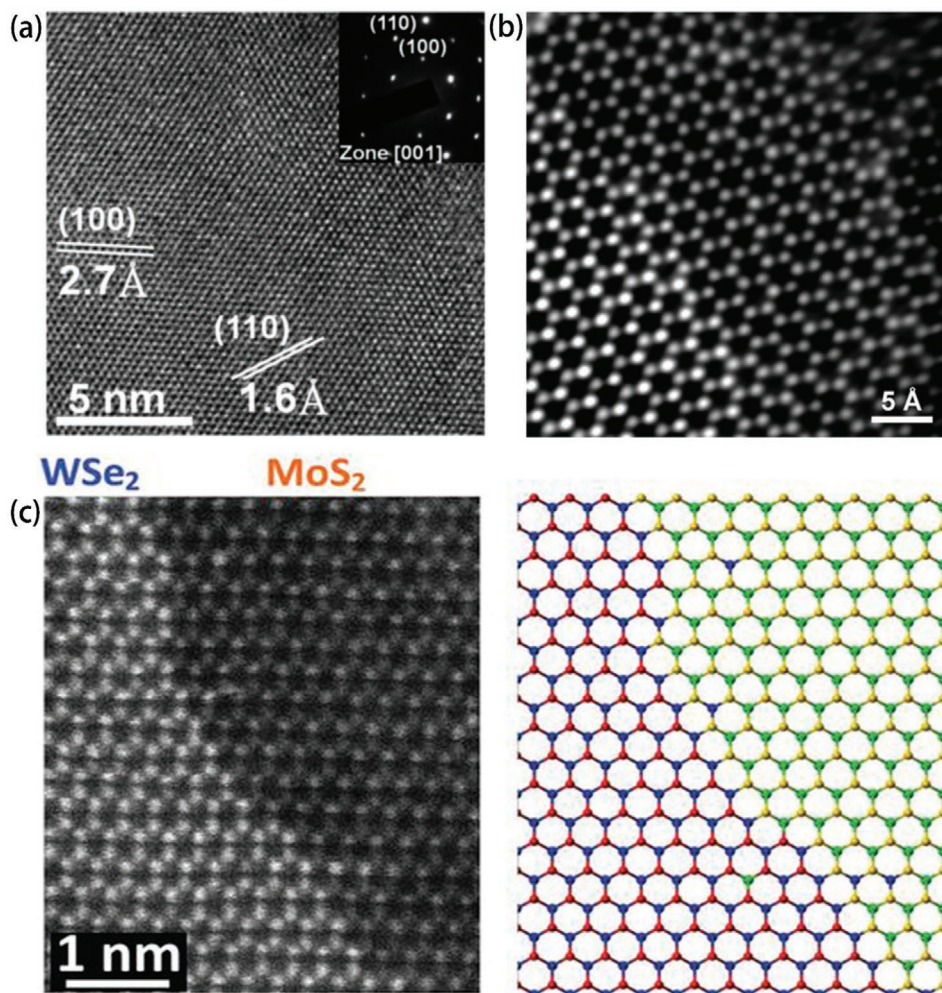


Figure 2. a) Surface topography and selected area electron diffraction pattern (inset) of MoS₂ in TEM image. Reproduced with permission.^[83] Copyright 2012, Wiley-VCH. b) STEM of single-layer MoS₂ with corresponding elements. Reproduced with permission.^[85] Copyright 2014, Wiley-VCH. c) STEM images of WSe₂-MoS₂ heterostructure. Reproduced with permission.^[86] Copyright 2015, American Association for the Advancement of Science.

The first exploration of Raman characteristics of ultrathin 2D TMDs dates back to 2010. Lee et al. reported the Raman spectra of thin and bulk MoS₂ films. As shown in Figure 5,^[94] not only

the two obvious vibrations out-of-plane (A_{1g}) and in-plane (E_{2g}^1) are observed, but also the shift tendency of two vibrations as the thickness changes are revealed. Moreover, the tension/stress

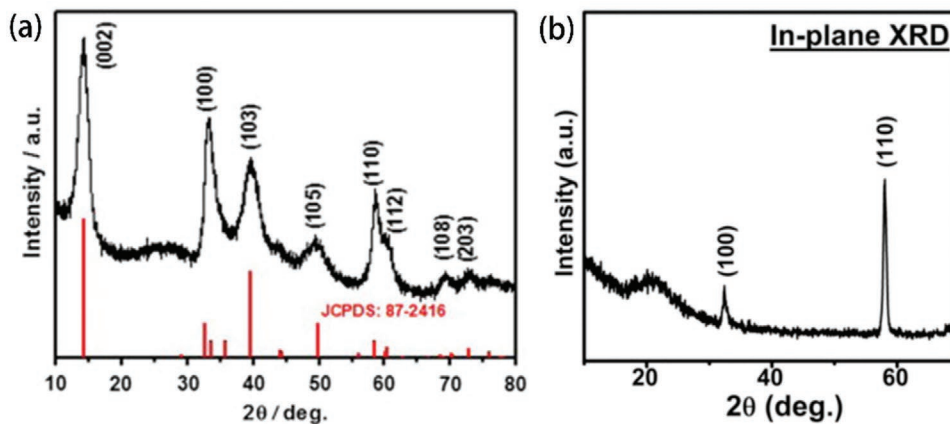


Figure 3. a) XRD for few layered MoS₂. Reproduced with permission.^[88] Copyright 2011, Elsevier Inc. b) XRD for monolayer MoS₂. Reproduced with permission.^[83] Copyright 2012, Wiley-VCH.

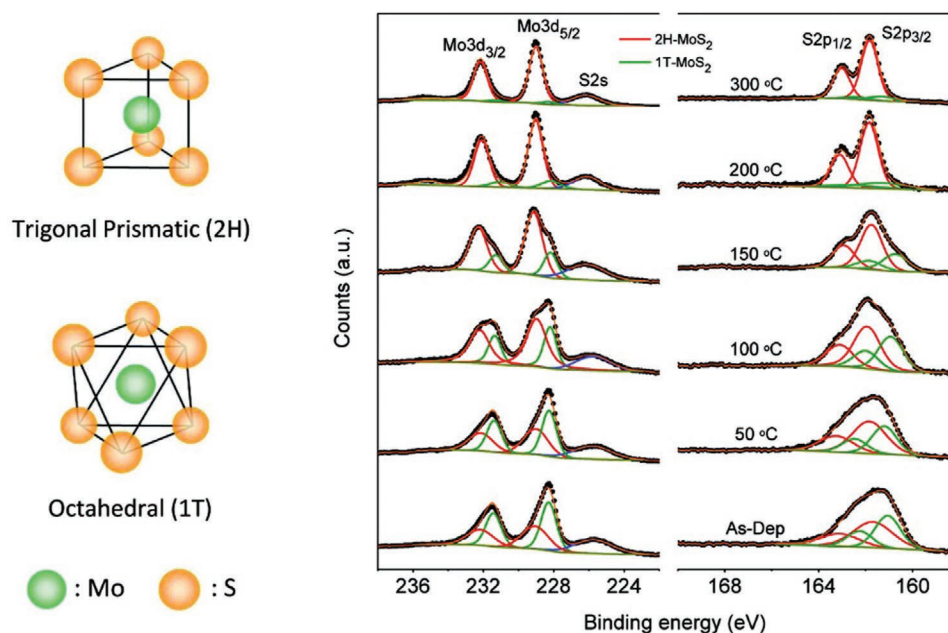


Figure 4. a) Atomic structure of 1T- and 2H-MoS₂. b) XPS of MoS₂ annealed at different temperatures. Reproduced with permission.^[92] Copyright 2011, American Chemical Society.

can be estimated by the peak position change of Raman, and the crystal symmetry and orientation are reflected by the Raman polarization energy.^[95] And for some special 2D materials (MoS₂ and WS₂), the layer information can be inferred by the distance of specific peaks on the Raman spectrum.^[96]

4. The Optical Properties of 2D Materials

4.1. Basic Properties of Several Common 2D Materials

2D materials commonly refer to crystals composed of few layers of or single atoms whose electrons move freely only on two dimensions of the non-nanometer scale (1–100nm). Although there have been a few investigations about 2D materials before, the rise of 2D materials has been

accompanied by the successful separation of graphene, a single-atom-layer graphite material, by Novoselov et al. in 2004.^[63] The following will introduce some materials that have been widely studied from the aspects of structure, bandgap, and so on.

Some of those materials are single element compounds or multielement compounds, so their atomic structures are different. The atomic structure of graphene is a hexagonal honeycomb lattice composed of carbon atoms as shown in Figure 6a.^[97] The atomic structure of black phosphorus is folded as shown in Figure 6b, which results in the high anisotropy of phonons, photons, and electrons.^[18,53,98] TIs are a group of materials with topological electronic properties, including antimony telluride (Sb₂Te₃), bismuth selenide (Bi₂Se₃), bismuth telluride (Bi₂Te₃), etc.^[99] Figure 6c shows the atomic structure of Sb₂Te₃, which is similar to the atomic structure of other materials in TI.^[100] The single-layer TMD structure can be

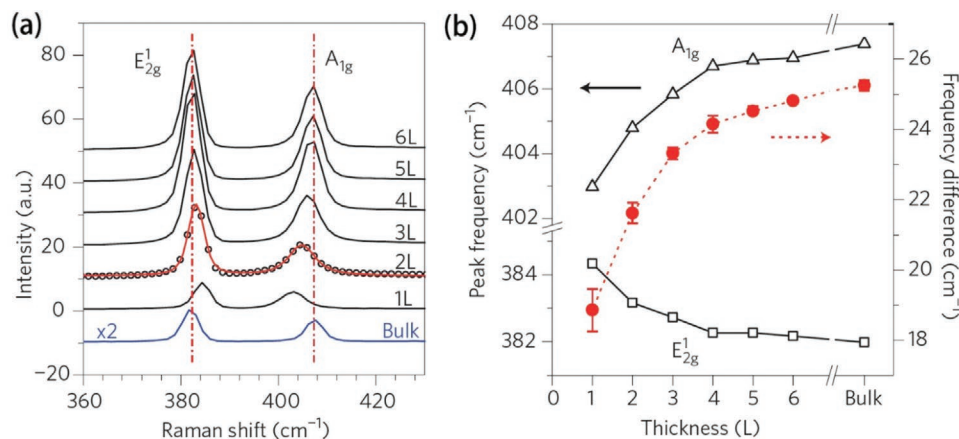


Figure 5. a) Raman spectroscopy of MoS₂ with different thickness. b) Variation of vibration mode with the thickness of MoS₂. Reproduced with permission.^[94] Copyright 2010, American Chemical Society.

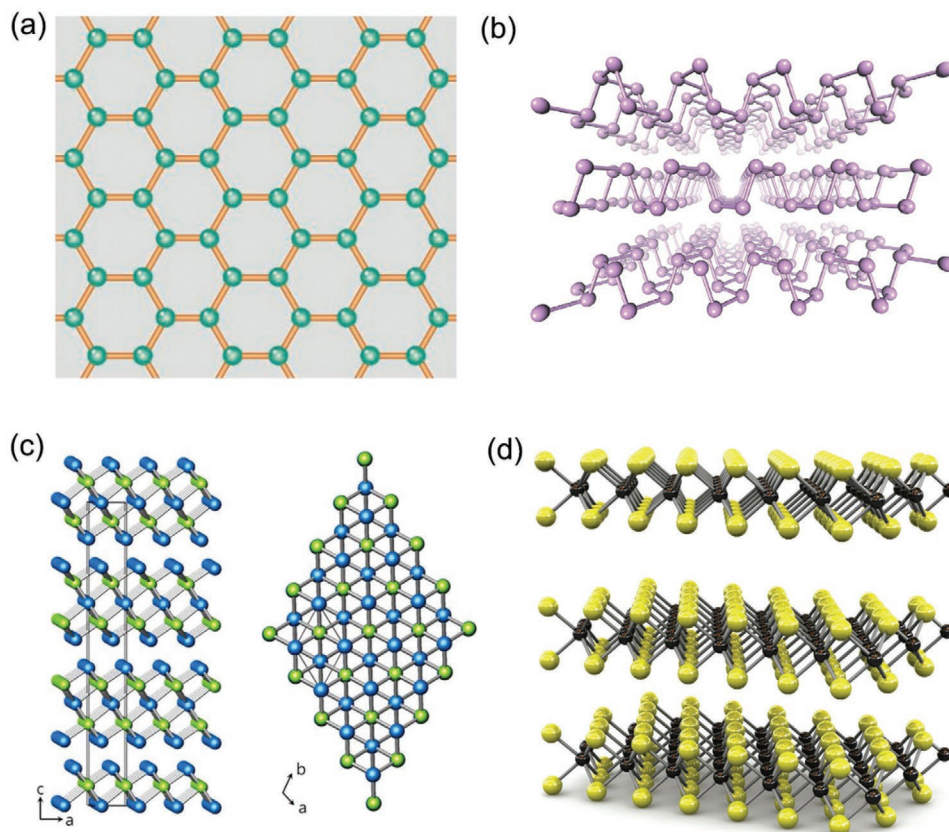


Figure 6. Atomic structure of a) Graphene. Reproduced with permission.^[97] Copyright 2010, American Association for the Advancement of Science. b) BP. Reproduced with permission.^[18] Copyright 2014, Springer Nature. c) TI (Sb_2Te_3). Reproduced with permission.^[100] Copyright 2017, IOP Publishing. d) TMD. Reproduced with permission.^[14] Copyright 2011, Springer Nature.

roughly represented by the three-layer atomic structure X–M–X as shown in Figure 6d, where the metal atom M from group 4 to 7 and chalcogen atom X is usually one of the three elements S, Se, and Te. In monolayer TMD, metal atoms M are sandwiched between two layers of chalcogen atom X, and the chemical bond M–X that provides the connection endows the whole layer strong stability, the thickness of which is usually 6–7 Å.^[14]

From the bandgap point of view, those materials have almost filled all the blanks of 0–2 eV. In graphene, the conduction band and valence band converge at the Dirac point, which indicates that graphene owns a gapless semimetallic band structure. TIs exhibit an insulating body state, and the surface state is Dirac electronic state with zero energy gap similar to graphene, which results in the metallic surface of the material. The metal properties exhibited on the edges and surface endow them small bandgap (0.2–0.3 eV). By adjusting the thickness, the bandgap value of BP will increase with the decrease of the number of layers in the range of 0.3–1.5 eV, but the bandgap of BP remains direct when the thickness changes. Compared with indirect bandgap materials, the electronic transition and recombination process in direct bandgap materials are easy, so the corresponding carrier lifetime is relatively short, which indicates that direct bandgap materials have advantages in realizing ultrashort pulses. Thickness-dependent bandgap structure is also one of the unique characteristics of TMDs. Taking MoS_2 as an example, the bandgap of bulk and monolayer MoS_2 are 1.29

and 1.80 eV. Meanwhile, with the decrease of thickness, the indirect bandgap of bulk MoS_2 changes into the direct bandgap of monolayer MoS_2 .^[12] Moreover, according to the inherent variation law of TMDS, when the chalcogen element gradually increases in atomic mass from S to Se to Te, the bandgap is synchronously reduced.^[101]

In addition, the unique properties of some materials need to be emphasized. For example, in graphene, a special quantum tunneling effect is followed by the carriers, which result in high carrier mobility and local superconductivity of graphene. Over a wide wavelength range, monolayer graphene exhibits an absorptivity of about 2.3%, which is better than traditional semiconductor materials such as gallium arsenide (GaAs) (about 1% absorption of near-gap light for a 10 nm thick GaAs quantum well).^[4] Moreover, in the range of at least 5 layers, the absorption increases by 2.3% for each layer increased in thickness.^[102,103] BP is easily oxidized and cannot be stably present in the air for a long time. In order to solve this problem, many packaging methods have been used for its long-term work and preparation, but the practical application is still challenging.

4.2. Kerr Effect and Saturable Absorption

In a high-intensity electromagnetic field, the response of some medium to light will become nonlinear. Therefore, the

exploration of the optical nonlinearity of 2D Materials is conducive to its further development in photonics and photoelectric applications.^[104–111] The origin of the nonlinear response of medium is related to the nonresonant motion of the bound electrons under the influence of the applied field. The induced total polarization P of the electric dipole is nonlinear to the optical field strength E , satisfying the relationship^[112,113]

$$P = \epsilon_0(\chi^{(1)} \cdot E + \chi^{(2)} : E + \chi^{(2)} : E + \dots) \quad (1)$$

In the formula, ϵ_0 is the dielectric constant in a vacuum and $\chi^{(n)}$ ($n = 1, 2, \dots$) is the n th-order of polarizability. First-order $\chi^{(1)}$ describes the linear response. Second-order $\chi^{(2)}$ corresponds to nonlinear effects including sum frequency and second harmonic generation, which is zero in some media with inverted symmetry of the molecular structure. The lowest order nonlinearity in optical fibers originates from third-order polarizability $\chi^{(3)}$, which is the cause of phenomena such as four-wave mixing, nonlinear refraction and third-harmonic generation. The real part of $\chi^{(3)}$ is related to the nonlinear refractive index of the material, which is called the Kerr effect, while the imaginary part represents the nonlinear absorption of the material. One of the most significant manifestations of the nonlinear absorption is the saturable absorption properties of materials.

For 2D materials, the Pauli exclusion principle is considered to be the main origin of saturable absorption,^[4,114] which can be briefly described as follows. When materials are illuminated by the weak light, the electrons in the valence band transits to the conduction band because of the absorption of photon energy. Subsequently, in-band phonon scattering will further “cool” these hot carriers until the equilibrium distribution of electrons and holes is restored, which is a linear absorption process. When the incident light is strong, the above-mentioned electronic transition process is frequent, and the energy states of the valence band and the conduction band edge are all occupied by electrons and holes. Since electrons are fermions, according to the Pauli exclusion principle, when all energy states are occupied, the interband transition will be cut off, and the material will no longer absorb photon energy, thus showing a state of low absorption and high transmittance. This saturable absorption process can be described as follows

$$\alpha = \alpha_{\text{ns}} + \frac{\alpha_s}{1 + I/I_{\text{sat}}} \quad (2)$$

where α_{ns} is nonsaturable loss, α_s is a saturable loss (modulation depth), I is the input intensity, and I_{sat} is the saturation intensity. Corresponding to the previous nonlinear absorption process, when the incident light is weak (I is small), the absorption is the sum of α_{ns} and α_s , and when the incident light becomes stronger, the absorption is reduced to α_{ns} .

In the measurements of saturable absorption and Kerr effect, the Z-scan technique and double-balanced detection are two commonly used methods.^[115–117] The device diagram of Z-scan technique is shown in **Figure 7**.^[118] Part of the incident Gaussian beam is separated by beam splitter and detected by detector 1 to monitor the stability of light intensity. The remaining part is focused by the lens, the focal plane of the

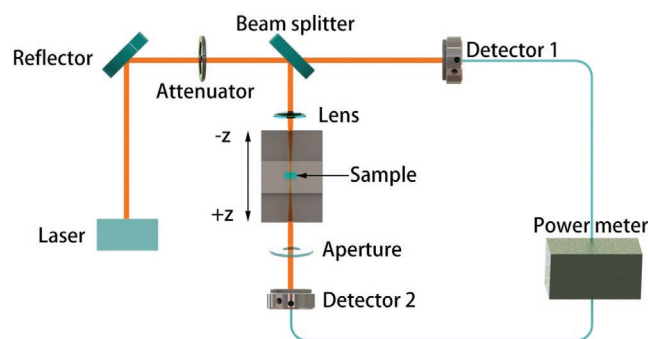


Figure 7. The schematic diagram of Z-scan measurement. Reproduced with permission.^[118] Copyright 2018, IOP Publishing.

focusing lens is located at $Z = 0$, and the direction of beam propagation is defined as $+Z$ direction. The measured sample is placed on the translation stage and can move around the focal plane. An appropriate aperture is placed before detector 2 to obtain the data of open-aperture (OA) and closed-aperture (CA) by changing the state of aperture, thus measurement is roughly divided into two processes. For OA Z-scan, due to the nonlinearity of the medium and the lateral spatial nonuniformity of the Gaussian beam, the sample moving around the focal point of the lens can be considered as a lens-like medium, which ultimately leads to the divergence or convergence of the beam, changing the lateral distribution of the far-field light field. Therefore, the intensity-dependent transmission and absorption coefficients are easy to get by comparing the intensity recorded by the two detectors (**Figure 8a**.^[119] For CA Z-scan, since the beam-induced refractive index of the material affects the beam diameter passing through it, the intensity recorded by detector 2 is affected by both the beam diameter after the sample and transmission of the sample.^[120] After synthesizing the OA and CA Z-scan data, the nonlinear refractive index and the real part of $\chi^{(3)}$ can be deduced as shown in **Figure 8b**.^[115,121] Z-scan measurement technology transforms the additional phase caused by material nonlinearity into the spatial variation of the amplitude of the light field to be measured by diffraction. Its appearance is important progress in the field of nonlinear measurement.

In addition to the Z-scan technique, the double-balance detection, as a simplified version, can also be used to measure the saturable absorption properties of materials. The schematic diagram of the double-balance detection method is shown in **Figure 9**.^[122] The mode-locked pulses are divided into two equal parts by the optical fiber coupler after passing through the variable attenuator. One of them is detected directly for a reference. Another one passes through the material before it is detected. By adjusting the variable attenuator, the intensity of light injected into the material is changed, and then the intensity-dependent absorption characteristics of the material are obtained by comparing data recorded from two detectors. Since the propagation of light is confined to the fiber in the measurement, the spatial information is absent unlike the Z-scan, this method can only be used to measure the intensity-dependent nonlinear absorption. However, because of its compact device and easy operation, it is still considered as one of the best choices in simple nonlinear measurement for 2D material.

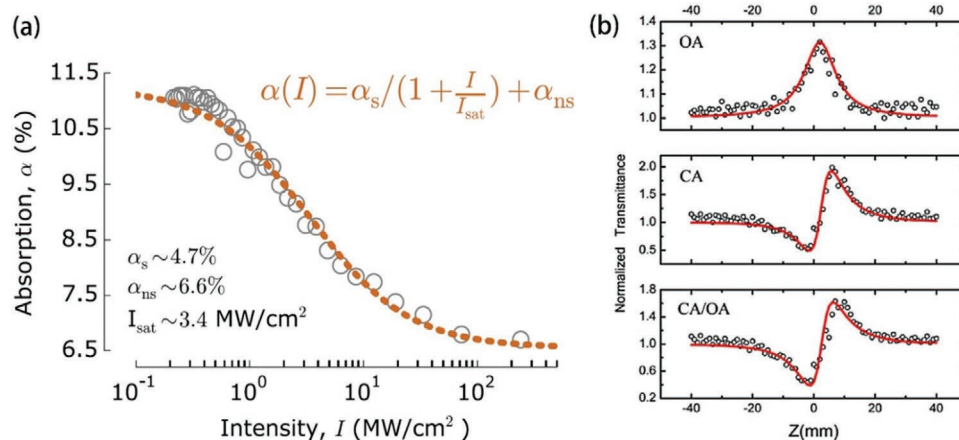


Figure 8. a) The nonlinear optical absorption measured by a Z-scan technique. Reproduced with permission.^[119] Copyright 2015, The Optical Society. b) The typical shapes of Z-scan measurements. Reproduced with permission.^[115] Copyright 2015, The Optical Society.

4.3. Coupling Structure of SAs

The fabricated 2D materials are thin sheets with small size and nanometer thickness, which cannot be directly applied to lasers. Therefore, it is necessary to couple materials into appropriate optical structures to facilitate the interaction between materials and light. This kind of photonic device with 2D materials and optical fiber structure is called SAs. So far, there have been some effective coupling structures, which can be roughly divided into several types as shown in **Figure 10**.^[75,119,123–126] In **Figure 10a**, 2D materials are directly filled the hollow channel of the photonic crystal fiber, which ensures sufficient material-light reaction. However, it is difficult to produce, and the coupling between photonic crystal fibers and single mode fibers is inconvenient. In **Figure 10b**, the 2D material sheets are sandwiched between two fiber connectors. Since the diameter of the fiber cores is only about 9 μm , a small piece of material can effectively ensure transmission coupling. This coupling method is simple and convenient, but the low damage threshold of which is difficult to deal with in application. On the one hand, the laser travels directly through the material for a long time. On the other hand, the tight coupling results in heat accumulation, so the material is easy to be damaged. Inspired by SESAM, materials are plated on the surface of gold/silver mirrors to

form reflective structures as shown in **Figure 10c**. However, when it is used in a fiber laser, the light from fiber connector needs to be perpendicular to the mirror surface, which is difficult in practical operation, and fiber connector inevitably causes damage to the mirror surface by rubbing. In order to avoid collimation and contact damage, some people directly coat the material and gold surface on the end of the optical fiber, but the reflection effect of the gold layer is not as good as that of gold/silver mirrors, and in serious cases, the light may overflow. By plating the material on the surface of the microfiber, the laser in the fiber can interact with the material without going straight through the material utilizing the evanescent field of the light and microfiber as shown in **Figure 10d**. In this way, the photo-synthetic material has a long acting time and avoids heat accumulation, but the microfiber is fragile and vulnerable, which is inconvenient for application and storage.

5. Fiber Laser Based on 2D Materials

In fiber lasers, there are two main methods to generate ultra-short pulses: Q-switching and mode-locking. The schematic diagram of the classical ring cavity is simple and convenient as shown in **Figure 11**.^[118] Different advantages make them more selective in the application. Because of the high peak power of Q-switched lasers, they are commonly used in laser processing and military. Mode-locked lasers are used in the fields of micromachining and nanoimaging because of their advantages in ultrafast laser. Below we introduce the relevant mode-locking and Q-switched lasers according to the types of materials.

5.1. Pulsed Lasers Based on Graphene

Duo to the unique photoelectric properties, graphene has received widespread attention and investigation since its inception.^[127] The application advantages of graphene in lasers are mainly in the broadband absorption, ultrafast photonics and high damage threshold. First, the conduction band and valence

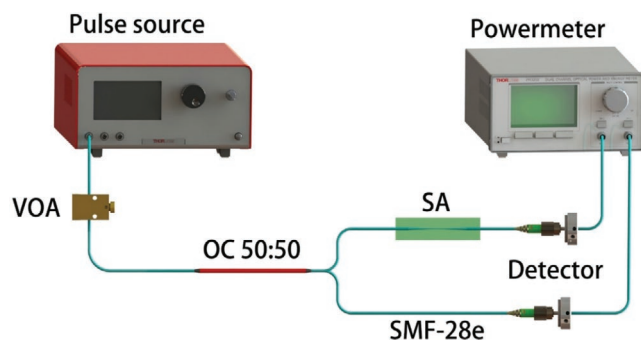


Figure 9. Schematic diagram of the double-balance detection method. Reproduced with permission.^[122] Copyright 2018, Chinese Physical Society and IOP Publishing.

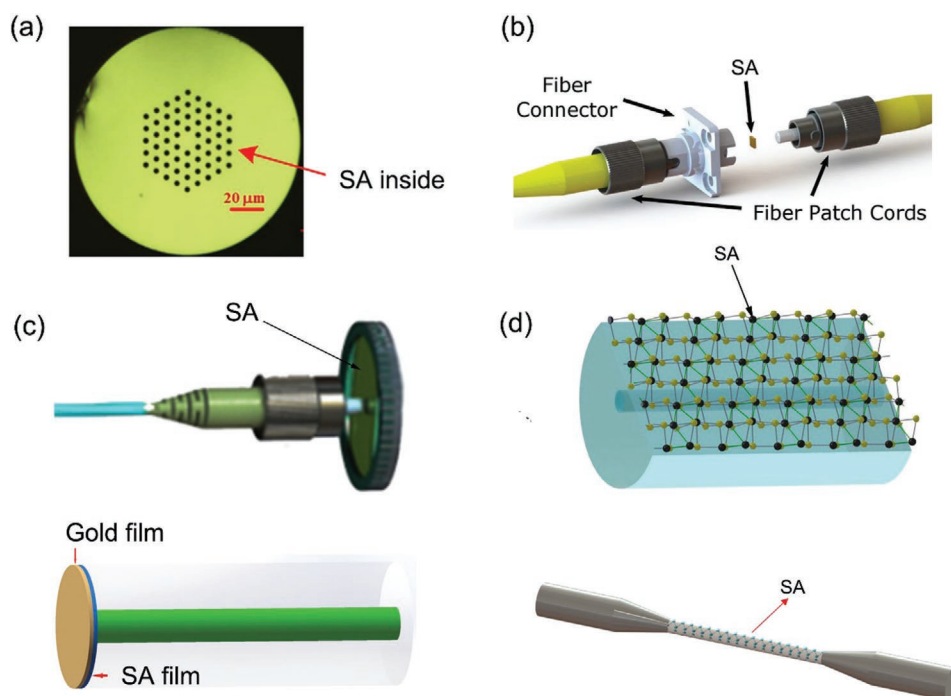


Figure 10. Coupling Structure of SAs. a) SA into hollow photonic crystal fibers (PCFs). Reproduced with permission.^[123] Copyright 2013, The Optical Society. b) SA sandwiched between two fiber connector. Reproduced with permission.^[119] Copyright 2015, The Optical Society. c) reflective structure: above is a saturable absorber mirror. Reproduced with permission.^[124] Copyright 2018, The Optical Society. Below is an optical fiber end coating. Reproduced under the terms of a Creative Commons Attribution License.^[75] Copyright 2016, Chen Hao. Published by SPIE. d) Microfibers: above is the D-type fibers. Reproduced with permission.^[125] Copyright 2017, Springer Nature. Below is the tapered fibers. Reproduced with permission.^[126] Copyright 2018, IOP Publishing.

band of graphene converge at the Dirac point, which indicates that graphene owns a gapless semimetallic band structure. This zero bandgap structure is conducive to broadband absorption of graphene. Second, high carrier mobility and fast relaxation time are achieved due to the special quantum tunneling effect of carriers in graphene. Bao et al. has measured the relaxation time of graphene with pump-probe experiments, and found that the fast relaxation time of graphene is about 150 fs.^[128] Their research shows that graphene with fast relaxation time is more effective in shaping ultrashort laser pulses. Finally, The melting point of graphene is up to 4125 K.^[129] In the experiment, graphene shows a high damage threshold, which is suitable for the application in a high power laser. So far, there have been pieces of research on graphene in fiber lasers.

The summary of graphene-based MLFLs achieved so far are shown in Table 1. The optical nonlinearity of graphene

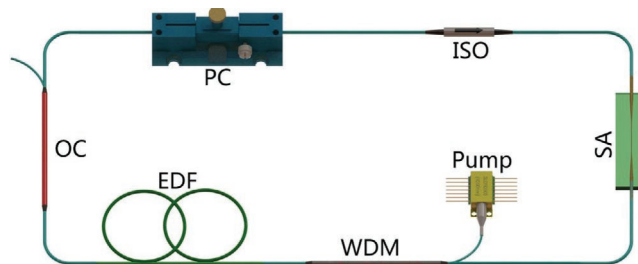


Figure 11. The schematic diagram of the classical ring fiber laser. Reproduced with permission.^[118] Copyright 2018, IOP Publishing.

was investigated for the first time by Bao et al.^[4] They not only theoretically discussed the absorption process of light in graphene in detail, but also measured the ultrafast relaxation process and the nonlinear absorption characteristics of graphene with different thicknesses. The prepared graphene SA was applied to the Erbium-doped fiber laser (EDFL), and stable mode-locked pulses at 1565 nm with 3 dB bandwidth of 5 nm were also obtained. The resulting optical soliton had a pulse duration of 756 fs as shown in Figure 12. This indicates that graphene can be used as ultrathin saturable material and has a great application prospect in ultrafast fiber lasers. Subsequently, Sobon et al. established an all-polarization maintaining graphene-based EDFL.^[133] The EDFL which operated at 1555 nm with 6 nm 3dB bandwidth had a pulse duration of 590 fs. Moreover, the measured polarization of the laser is 93.5%, and the azimuth and resolution changes are small. Fu et al. realized three different lasers (Tm: Ho-, Er-, and Yb-doped lasers) based on graphene with a wavelength span of more than 1000 nm,^[139] which illustrated the broadband absorption capacity of graphene. Based on graphene SA, mode-locked optical solitons with a pulse duration down to 88 fs have been obtained by Sotor et al.,^[142] which is considered to be the best in graphene-based lasers to the best of our knowledge. The corresponding average output power (AOP) and pulse energy (PE) were 1.5 mW and 71 pJ, respectively. Pawliszewska et al. have demonstrated a holmium-doped laser operating at 2060 nm with 53.6 nm 3dB bandwidth.^[143] The mode-locked system with 190 fs pulse duration reaches

Table 1. Performance summary of MLFLs based on graphene.

Materials	MD [%]	Repetition frequency [MHz]	λ [nm]/ $\Delta\lambda$	Pulse duration [fs]	SNR [dB]	Mode-locked threshold [mW]	Power [mW]	Maximum pulse energy [nJ]	Ref.
Graphene	–	6.46	1940	3600	–	–	2	0.4	[130]
	2.93	25.67	1559.12/6.16	432.47	31	53.3	–	0.09	[131]
	32	6.22	1566/4.92	880	65	18	–	–	[132]
	66	–	1565/1.5	2100	–	–	–	–	[55]
	3.6	45.88	1555/6	590	70	38	0.91	–	[133]
	<0.4	20.5	1884/4	1200	–	–	1.35	–	[134]
	12.88	27	1546/0.2	26000	>70	–	–	–	[135]
	8.4	106	1560/2.7	900	–	25	9.6	–	[136]
	–	25	2784.5/0.21	39000	43.5	420	18	–	[137]
	–	12.8	1953.3/2.2	2100	50	130	1.41	–	[138]
	2.7	19.3	1564/3.15	870	64	47	–	0.0104	[139]
	–	1.82	1908/0.26	6.5×10^7	65	580	–	0.0162	[139]
	–	16.29	1035/0.18	6.5×10^6	55	249	–	0.81	[139]
	5.5	38.45	1939.6/6.8	654	77	–	–	–	[140]
	0.2	37.72	1607.7/8.6	377	66.6	–	5.41	–	[141]
	11	21.15	1545/48	88	65	80	1.5	0.071	[142]
	12	20.98	2060/53.6	190	65	–	54	2.55	[143]
–	–	1570–1600/7.2	49000	–	–	–	2.3	[144]	
66.50	1.79	1565/5	765	65	8	–	–	[4]	
–	8	1553/3	1000	80	20	1	0.125	[145]	

2.55 nJ of PE. The AOP was 54 mW, which is also optimal for similar lasers in Table 1.

The summary of graphene-based Q-switched fiber lasers (QSFLs) achieved so far are shown in Table 2. For the first time, Luo et al achieved a graphene-based QSFL in 2010.^[146] The pulse duration and PE of observed Q-switched pulses were 3.7 μ s and 16.7 nJ. In addition, the laser exhibits spectral response both at 1566.17 and 1566.35 nm. It is also pointed out that the stable operation of this dual-wavelength laser is mainly attributed to the elimination of mode competition in EDF due to the strong optical nonlinearity of graphene. In 2011, the Q-switched pulses were observed in Yb-doped fiber laser (YDFL) which employed a graphene-based saturable absorber mirror by Liu et al.^[149] The produced stable pulses exhibited a pulse duration of 70 ns,^[149] which is the shortest in graphene-based QSFLs. The next year, a graphene-based Q-switched thulium-doped fiber laser was demonstrated by Liu et al. for the first time, the generated stable pulse with a center wavelength of 2 μ m and short pulse duration of 1.4 μ s. The single PE is 85 nJ.^[151] Based on graphene SA, Yap et al. established a QSFL with a linear cavity configuration.^[152] The laser was centered at 1535 nm with a 3dB wavelength of 0.268 nm. The AOP was 20 mW. The PE up to 184 nJ is the best in Table 2.

Although graphene-based lasers have been greatly developed, with the deepening of research, some shortcomings of graphene have gradually been exposed. First, The low modulation depth resulted from its low absorption efficiency (2.3% per layer) restraint its further applications in laser.^[158] Although the modulation depth of graphene can be increased by increasing the number of graphene layers, it also adds a lot of additional unsaturated loss, so that the laser performance

is reduced.^[128] Second, the saturation threshold of graphene varies with the operating wavelength. When the operating wavelength is shorter, the saturation threshold of graphene is larger. It indicates that graphene is more suitable for working in the mid-infrared band, and the working performance in the short wavelength band is slightly worse.^[159,160]

5.2. Pulsed Lasers Based on TIs

TIs are a general term for a class of materials with topological electronic properties.^[161] This kind of material has an insulating body state, and the surface state has a Dirac electronic state with zero energy gap similar to graphene, which leads to the metallic surface of the material. Generally, the bandgap of TIs is 0.2–0.3 eV, which means that they can show saturable absorption characteristics when the wavelength is less than 4.2 μ m. This wide spectral range already covers most of the important bands. In addition, TIs generally have a high nonlinear refractive index and modulation depth. It has been reported that the modulation depth of TI (Bi_2Te_3) at 1570 nm is more than 70%, which is higher than that of most 2D materials.^[105] Meanwhile, TIs also possess large nonlinear refractive index from Z-scan measurements.^[104] Lu et al. have reported that third-order optical nonlinear refractive index of TI: Bi_2Se_3 is up to $10^{-14} \text{ m}^2 \text{ W}^{-1}$. Therefore, they can not only provide high nonlinearity for the cavity, but also obtain narrow pulse duration due to the high modulation depth, thus can be used as ideal SAs in fiber lasers.

As early as 2012, Bernard et al. proved the optical nonlinearity of Bi_2Te_3 by measuring the power changes before and

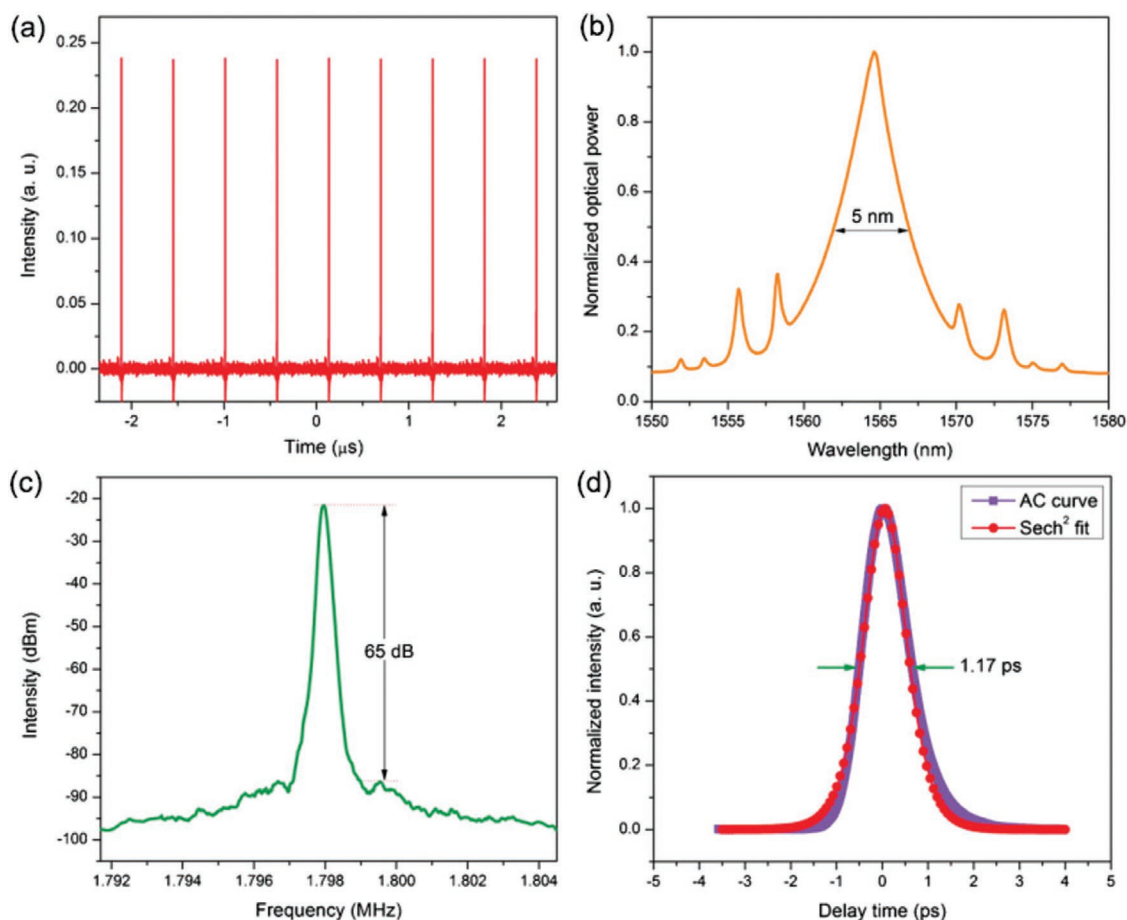


Figure 12. Performance of MLFL based on graphene SA. a) Pulse trains; b) the spectrum; c) RF spectrum; d) intensity autocorrelation trace. Reproduced with permission.^[4] Copyright 2009, Wiley-VCH.

after the material, and predicted that it could be used as SA in lasers.^[162] Since then, laser research based on TIs has been booming and has made great achievements. The performance

of TIs in MLFLs are summarized in **Table 3**. Zhao et al. obtained mode-locked pulses using TI SA (Bi_2Te_3) for the first time.^[164] The prepared Bi_2Te_3 SA has a modulation depth (MD) of up to

Table 2. Performance summary of QSFLs based on the graphene.

Materials	MD [%]	Repetition frequency [kHz]	λ [nm]/ $\Delta\lambda$	Pulse duration [ns]	SNR [dB]	Mode-locked threshold [mW]	Power [mW]	Maximum pulse energy [nJ]	Ref.
Graphene	45	3.3–69.5	1566.17/0.04 1566.35/0.04	3700	–	6.5	1.1	16.7	[146]
–	–	67	1557/0.3	2000	–	74	2.4	40	[147]
–	–	3.2–9.7	1519.3–1569.9/–	4600	–	33	0.032–1.192	82.61	[148]
–	–	140–257	1064.2/0.13	70	–	120	12	46	[149]
–	–	22.8	1531.12/0.18	8200	–	120	–	70.2	[150]
–	8	53	2007.1/0.1	1400	40	1250	4.5	85	[151]
–	–	20	1535/0.268	5900	–	25	20	184	[152]
–	–	115	1560–1570/–	1850	–	120	175	125	[153]
–	–	236.3	–/–/–	206	–	16.9	7.8	33.2	[154]
–	–	26	1884/–	2300	–	320	1.8	70	[155]
–	–	135.7	1560/–	185	–	–	–	–	[156]
–	–	23.96	1060/–	18790	–	181	–	–	[157]

Table 3. Performance summary of MLFLs based on the TI.

Materials	MD [%]	Repetition frequency [MHz]	λ [nm]/ $\Delta\lambda$	Pulse duration [fs]	SNR [dB]	Mode-locked threshold [mW]	Power [mW]	Maximum pulse energy [nJ]	Ref.
Bi ₂ Te ₃ (n-)	13.3		1570/6.56	400	–	–	–	–	[163]
Bi ₂ Te ₃ (p-)	11		1575/6.92	385	–	–	–	–	[163]
Bi ₂ Te ₃	95.3	1.21	1558.4/2.69	1210	–	70	–	–	[164]
	1.8	1.44	1057.82/3.69	230000	77	200	0.86	0.599	[165]
	15.7	15.11	1547/4.63	600	65	55	0.8	–	[166]
	20.6	27.9	1935/5.64	795	76	–	–	–	[167]
	19.1	1.11	1064.47/1.11	960000	60	74	1.2	–	[168]
	9.8	21.5	1909.5/3.43	1260	52	315	–	–	[169]
	2	8.635	1557/2.9	1080	>60	13	0.4	–	[170]
	4.8	232.14	1564/2.1	1320	60	80	5.3	–	[171]
		10.4	2830/10.1	6000	–	680	90	8.6	[172]
		27	28.5	–/2.86	403	–	–	–	–
Bi ₂ Se ₃	11.05	16	1038.5/–	380000	35	175	17.1	1.06	[174]
	39.8	23.3	1562.4/4.28	630	51	69.2	–	0.0156	[175]
	14.5	0.527	1065.8/0.025	3.98 × 10 ⁸	>40	105	32.6	61.8	[176]
	6.9	0.5376	1562.27/0.265	1.87 × 10 ⁸	56	–	9.23	17.2	[177]
	3.8	8.83	–	22000	55	–	9.7	1.1	[178]
	5.2	35.45	1600/7.9	360	>56	145	0.86	–	[179]
	3.4	9.75	1566.6/0.25	–	75	200	–	–	[180]
	4.3	7.04	1610/1.06	2760	35	1200	308	–	[181]
	98	1.21	1564.6/1.79	1570	–	65	–	–	[182]
	3.9	12.5	1557.5/4.3	660	>55	25	1.8	0.144	[47]
	5.2	44.6	1031.7/2.5	46000	58	153	33.7	0.756	[183]
	13.4	18.37	1912.12/4.87	853	65	200	–	–	[184]
	Sb ₂ Te ₃	6	22.32	1565/30	128	65	80	1	0.0448
6		38.54	1561/10.3	270	70	30	–	0.029	[186]
3.9		22.13	1556/6	449	74	44	0.9	0.0396	[187]
–		4.75	1558.6/1.8	1800	60	45	0.5	0.105	[188]
1.5		50	1562.82/3.75	100	>77	108	5.09	0.0482	[189]
38		14.52	1930.07/3.87	1240	84	400	130	8.96	[190]
2.9		19.28	1047.1/8.78	5900	71	–	4	0.21	[191]
6		22.4	1564/8.5	125	65	28	–	–	[192]
–		39.5	1945/4.5	890	60	530	1.2	0.03	[193]
7.42		95.4	1542/63	70	65	91	31.5	–	[194]

95%, which further illustrates the optical nonlinearity of TIs. By using Bi₂Te₃ as a SA, Haris et al. experimentally demonstrated a mode-locked EDFL.^[175] The pulse duration of which was 0.63 ps. Liu et al. also reported the generation of the ultrashort pulses in EDFLs based on Bi₂Se₃ SA.^[47] The MD of the composite film is 3.9%. Then, by optimizing the cavity parameters, ≈660 fs optical pulses with a center wavelength of 1557.5 nm were generated. Sb₂Te₃, also a type of TIs, has attracted widespread attention. For the first time, Sotor et al. demonstrated an EDFL, which uses Sb₂Te₃ SA to achieve effective mode-locking.^[188] The stable optical soliton was centered at 1565 nm with 3 dB bandwidth of 1.8 nm. The measured pulse duration was 1.8 ps. Subsequently, they produced a mode-locked fiber laser with stretched pulses

based on Sb₂Te₃,^[185] the MD of prepared Sb₂Te₃ SA is 6%, which is sufficient for the generation of pulse mode-locking. With the Sb₂Te₃ SA with a side-polished fiber structure, the resulting laser was capable of producing mode-locked pulses centered at 1565 nm with 3dB bandwidth of 30 nm. The pulse duration of 128 fs obtained was the shortest one at that time. In 2016, a hybrid mode-locking method based on Sb₂Te₃ was proposed by Liu et al.^[194] The Sb₂Te₃ SA was fabricated by a pulsed laser deposition method, the MD of which was 7.42%. Combining the nonlinear polarization evolution with Sb₂Te₃ SA, the stable mode-locked pulses with a central wavelength of 1542 nm and 3 dB spectral width of 63nm were observed. The pulse duration of achieved mode-locked was as short as 70 fs as shown

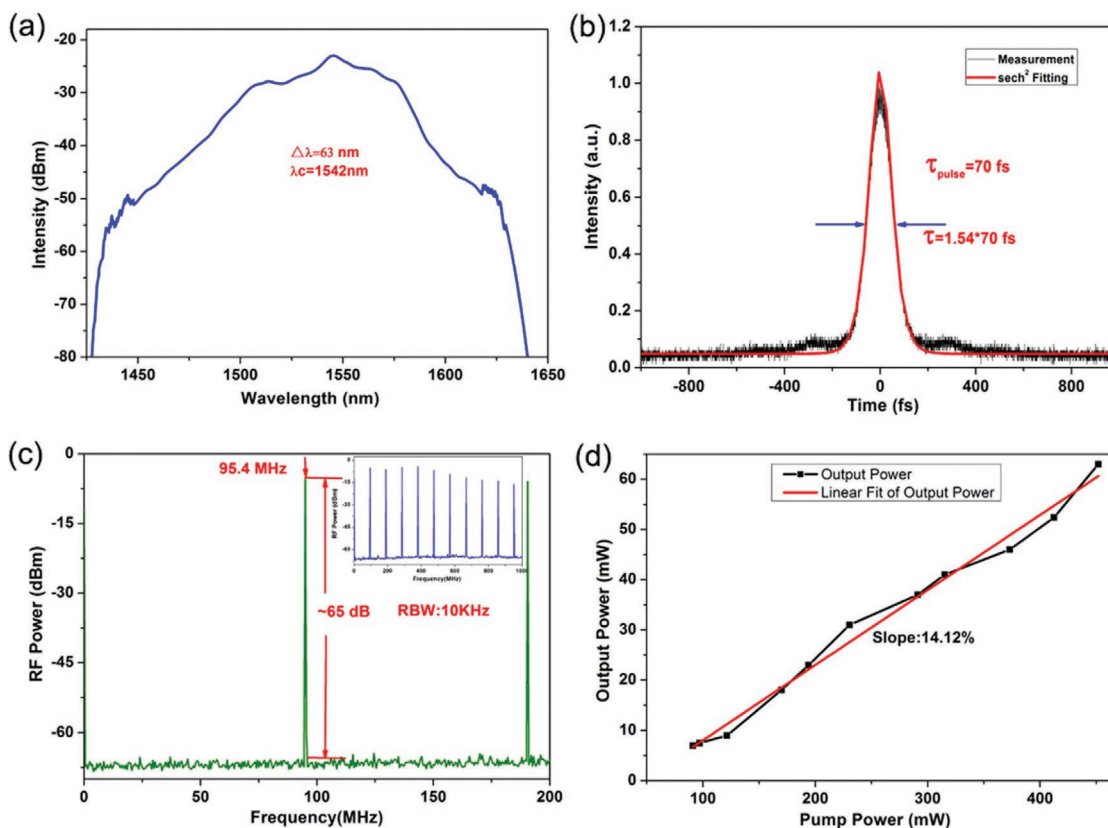


Figure 13. Performance of MLFL based on Sb_2Te_3 SA. a) The spectrum; b) intensity autocorrelation trace; c) RF spectrum; d) output power at different pump power. Reproduced with permission.^[194] Copyright 2016, Springer Nature.

Table 4. Performance summary of QSFLs based on the TI.

Materials	MD [%]	Repetition frequency [kHz]	λ [nm]/ $\Delta\lambda$	Pulse duration [ns]	SNR [dB]	Mode-locked threshold [mW]	Power [mW]	Maximum pulse energy [nJ]	Ref.
Bi_2Te_3	2.5/-/-	77	1056.5/0.8	1000	-	114	2.95	38.3	[195]
	7.7	60	1893/5.89	1710	-	175	0.68	11.54	[196]
	-	49.4	1557.5/0.04	3710	-	103.5	-	-	[197]
	10.8	42.8	1562.9/2	2810	-	17.3	0.55	12.7	[198]
Bi_2Se_3	11.05/-/17.4	137.8	-/-	2200	-	105	-	34.2	[174]
	-/-/-	205.2	1065.8/1.82	601	43	50	6.6	38.8	[199]
	15.7/46/81.1	-	1549.99/0.048	1340	-	80	23.61	224.5	[200]
	5/-/1.8	212	1550.49/0.02	2540	48	54.1	-	-	[201]
	39.8/-/90.2	68.2	-	2400	-	52.8	3.39	47.1	[175]
	7.7/-/-	86	2015.42/0.05	-	52	3100	195	3000	[202]
	-/-/-	195.3	1360.61/0.068	1520	-	140	56.1	111.2	[203]
	-/-/-	45.41	1036.72/-	1310	-	122.2	-	5.88	[204]
Sb_2Te_3	11.1/	36.6	1530/0.017	7600	-	60	-	6.1	[205]
	39.8/-/90.2	62.5	1560.33/-	2100	-	56	1.15	2.104	[206]
	3.8/-/53	29.1	1067.66/0.1	1950	48	42.5	0.46	17.9	[72]
	-	88.4	1531/4.68	4580	55	39.2	0.26	2.78	[207]
	-	132	1559/3	857	-	48	18.06	152	[208]
	6.2	338	1540.1/0.6	400	-	25	6.11	18.07	[209]

in **Figure 13**. This is not only the first successful application of hybrid mode-locking, as far as we know, but the resulting pulse duration of 70 fs is also the shortest one based on the SAs at the time.

The summary of TIs-based QSFLs achieved so far are shown in **Table 4**. A ytterbium-doped QSFL based on few-layer TI (Bi_2Se_3) was realized by Luo et al. for the first time.^[72] The stable Q-switched operation at 1.06 μm indicated the broadband saturable absorption of TI (like graphene). Recently, Zhang et al. realized Q-switched pulses which could be tuned from 1935.42 to 2048.85 nm with TI (Bi_2Se_3),^[202] which indicated that TI (Bi_2Se_3) exhibits great saturable absorption properties in the range of 1–2 μm , and further proves its broadband absorption capacity. Meanwhile, the realized laser performs well in high power. The AOP of Q-switched pulses was as high as 195 mW, which is the maximum value realized by SA in fiber lasers as far as we know. The corresponding PE of achieved Q-switched operation was up to 3 μJ . Yan et al. realized a QSFL based on the TI (Bi_2Te_3) SA which centered at 1557.5 nm.^[197] With the change of pump power, the pulse duration was adjusted in the range from 5.15 to 3.71 μs . Based on this laser, a cylindrical vector beam was obtained by mode selection of the Bragg grating. With a high-reflective TI (Sb_2Te_3) saturable absorber mirror (SAM), Yan et al. also demonstrated a wideband-tunable QSFL.^[209] The MD of Sb_2Te_3 SAM was measured as 6.2%. The pulse duration was 400 ns, which is the shortest among QSFLs based on TI SA. The central wavelength of achieved QSFL can be adjusted from 1530 to 1570 nm.

TIs have impressive optical nonlinearity, and have made a lot of achievements in laser applications, however, there are still some disadvantages. Although the nonlinearity of TI is better than that of graphene, its relaxation time is not as fast

as that of graphene, which indicates that TI is a slow saturable absorption material compared with graphene. In addition, as a chemical compound of two different elements, the preparation process of TI is relatively complex. Meanwhile, under normal experimental conditions, the SAs based on TIs show lower damage threshold. Some researchers have proposed that the damage threshold of SA may be increased by selecting the appropriate SA structure.^[181]

5.3. Pulsed Lasers Based on BP

As early as 2015, the electro-optical properties of black phosphorus began to arouse widespread interest.^[210] Unlike graphene and TIs, which are almost gapless, the bandgap of BP is adjustable by thickness.^[211] Due to the interaction between layers, the bandgap of BP decreases with the increase of thickness. When BP is bulk, its bandgap is down to 0.3 eV, therefore it is a very promising candidate for near-infrared and mid-infrared SAs. It is worth mentioning that no matter how the thickness changes, BP always maintains a direct bandgap, thus ensuring ultrafast electronic relaxation performance. Wang et al. has reported that the relaxation time was faster than that of graphene in the near-infrared and mid-infrared region by pump-probe experiments, which indicated that the pulse narrowing ability of BP is stronger than that of graphene.^[212] Therefore, the direct bandgap of BP is quite beneficial to the application of ultrafast photonics and high-frequency photonics. In recent years, lots of BPs-based MLFLs/QSFLs have been successfully established.

The MLFLs based on BPs are shown in **Table 5**. SA based on BP has been successfully fabricated by Chen et al. and applied

Table 5. Performance summary of MDFLs based on BP.

Materials	MD [%]	Repetition frequency [MHz]	λ [nm]/ $\Delta\lambda$	Pulse duration [fs]	SNR [dB]	Mode-locked threshold [mW]	Power [mW]	Maximum pulse energy [nJ]	Ref.
BP	8.1	5.96	1571.45/2.9	946	70	63.7	–	–	[213]
	9	9.46	1556.5/3.39	940	>50	30	5.6	–	[214]
	0.6	28.2	1560.5/10.2	272	65	80	0.5	–	[215]
	8	13.5	1085.58/0.23	7540	45	816	80	5.93	[216]
	50–90	14.7	1885.7/6.2	786	>50	–	1.6	–	[217]
	3.31	15.59	1558.14/1.25	2180	69.8	–	–	–	[218]
	21	8.77	1559.5/3.8	670	60	200	–	–	[219]
	9.8	19.2	1898/3.9	1580	–	303	8.45	–	[220]
	10.1	60.5	1569.24/9.35	280	68	95	–	–	[221]
	7	6.88	1560.7/6.4	570	59	30	5.1	0.74	[222]
	–	3.82	1558.8/14.2	805	–	–	–	–	[223]
	0.67	29.1	2094/4.2	1300	55	750	11	0.379	[224]
	10.03	23.9	1555/40	102	>60	34	1.7	0.071	[225]
	8.5	46.3	1030.6/0.11	<400000	49	200	32.5	–	[226]
	4.48	1.843	1568.19/0.52	1.176×10^8	>54	60	4.43	–	[227]
	16	12.5	1562/4.5	635	60	63	–	–	[6]
–	45.9	1558/48	100	>60	236	–	0.14	[228]	
–	36.8	1910/5.8	739	70	300	1.5	0.0407	[229]	

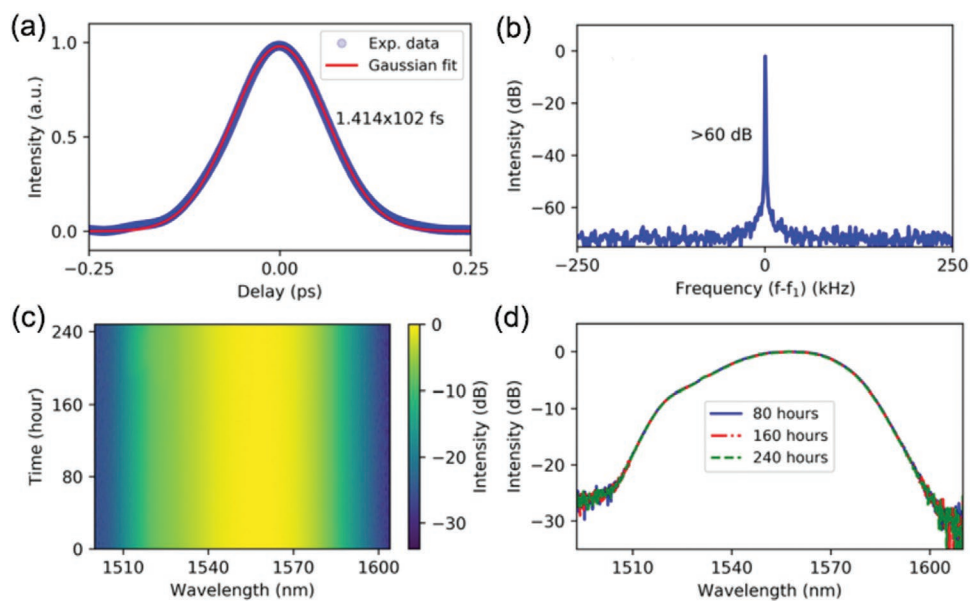


Figure 14. Performance of MLFL based on BP SA. a) Intensity autocorrelation trace; b) RF spectrum; c) spectra of long-term stable operation over 240 h; d) the spectrum. Reproduced with permission.^[225] Copyright 2018, The Optical Society.

in lasers to obtain stable mode-locked pulses, which is the first application of BP as SA in lasers.^[213] The mode-locked operation which centered at 1571.45 nm with a 3 dB bandwidth of 2.9 nm owns the pulse duration of 946 fs. The SNR up to 70 dB shows the stability of the system. Following this report, Sotor et al. demonstrated the polarization sensitivity of BPs SA.^[215] The fiber laser is mode-locked by a fabricated device based on BP. The generated optical solitons which centered at 1550 nm with 3 dB bandwidth of 10.2 nm had the pulse duration of 272 fs. In addition to the communication band, SAs based on BP were also investigated in wider bands. Hisyam et al. achieved the application of BP around 1 μm in YDFL.^[216] The pulse duration of generated optical solitons was 7.54 ps. The AOP of the laser was 80 mW, which is the maximum in a BP-based laser. The corresponding PE was 5.93 nJ. Pawliszewska et al. achieved the application of BP around 2 μm in a holmium-doped all-fiber laser.^[224] The generated solitons with a pulse duration of 1.3 ps were centered at 2094 nm with a bandwidth of 4.2 nm. So far, BP has been successfully applied in the range of 1–2 μm , indicating the broadband absorption characteristics of BP. The laser based on BP which with the shortest pulse was established by Jin et al.^[225] The BP SA used the experiment was manufactured by a scalable and highly controllable inkjet printing technology. The pulse duration of generated solitons was as short as 102 fs with a central wavelength of 1555 nm and 3 dB bandwidth of 40 nm as shown in Figure 14.

The QSFLs based on BPs are enumerated in Table 6. Among them, the maximum PE and shortest pulse duration were obtained by Yu et al.^[231] The BP-SA which with the MD of 24% was inserted in a thulium/holmium-doped fiber laser for Q-switched pulses. After proper pump power regulation, stable Q-switched pulses operating at 1912 nm with a bandwidth of 0.8 nm were presented. The shortest pulse duration of this Q-switched system was 731 ns. The maximum AOP and PE of the system were 71.7 mW and 632.4 nJ, respectively.

The broadband absorption characteristics of BP were also reflected in QSFLs. Jiang et al. simultaneously realized the application of bulk-structured BP at the 1.5 and 2 μm wavelengths.^[233] The BP SA was prepared by depositing the material on the side-polished single-mode fiber. For the QSFL operating at 1550 nm, the pulse duration was adjusted in the range of 9.35–31 μs . For the QSFL which operating around 2 μm , the operating wavelength was tuned from 1935 to 1832 nm at different pump power. Wang et al. prepared a BP SA with an MD up to 40.2% by depositing the material on a tapered fiber.^[236] Based on this BP SA, the pulse duration and PE of the Q-switched pulses were 5.6 μs and 154.2 nJ, respectively. Wang et al. experimentally investigated the performance differences of two BP-SA which with different structures in lasers. The laser based on BP SA with tapered fiber represented the narrower pulse duration of 1.09 μs and a higher repetition rate of 101.3 kHz, which indicates that the small taper diameter of tapered fiber can promote the interaction between materials and evanescent fields.^[238]

According to the current research, BP seems to show excellent broadband absorption characteristics and pulse duration narrowing ability, which can be considered as an ideal candidate for SAs, but its environmental instability is a major problem to be overcome. When BP was exposed to the air, it was found to have a fairly strong affinity for water, and its volume increased by more than 200% within several days due to water absorption. In addition, if it was exposed to the air for a long time, the surface of BP will be corroded layer by layer.^[242] This kind of environmental instability undoubtedly has a great influence on its optical properties, thus affecting the performance of saturable absorption devices based on BP. In addition, the thermal effect and optical damage caused by high power illumination will accelerate the damage of BP in the air, which also limits its application in high power laser.^[214] Although there are some ways to package it to avoid the direct contact of air, so

Table 6. Performance summary of QSFLs based on BP.

Materials	MD [%]	Repetition frequency [kHz]	λ [nm]/ $\Delta\lambda$	Pulse duration [ns]	SNR [dB]	Mode-locked threshold [mW]	Power [mW]	Maximum pulse energy [nJ]	Ref.
BP	18.55	10.42	1562.87/0.2	13200	45	35	–	94.3	[213]
	10.6	23.48	1561.9/1.5	4350	53	25	6.67	194	[230]
	24	113.3	1912/0.8	731	32.8	293	71.7	632.4	[231]
	–	40	1532.5/3	3160	56	23	0.728	18.6	[217]
	73	58.73	1038.68/–	1160	–	115.2	0.12	2.09	[232]
	–	4.43–18	1550/0.15	9350–31000	50	10.4	–	28.3	[233]
	–	26.4–73	1860/0.13	3100–4200	–	–	–	80.8	[233]
	–	24–57.2	1890/0.12	2530–4800	–	–	–	276	[233]
	–	14–60	1920/0.18	3000–4700	–	–	–	238	[233]
	73	27.2	1056.6–1083.3/–	4000	58	129.4	–	7.1	[234]
	7	32.9	1069.4/1.0	10800	40	55.1	–	328	[235]
	40.2	28.1	1948.2/1.94	5600	40.8	1010	3.8	154.2	[242]
	0.47	31.07	1556.93/2.66	3590	–	31.78	4.2	142.6	[237]
	15.75	79.46	1029.63/0.6	1550	–	95	–	165.11	[238]
	–	101.3	1030.72–1034.4/	1090	–	–	–	114.72	[238]
	–	17.2	1064.7/0.15	5720	35	–	–	–	[239]
	–	24.59	1060.1/0.09	4210	37	318	9.95	404.6	[240]
2.5	63	1040.5–1044.6/–	2500	30	220	8.9	141.27	[241]	

as to prolong its service life, the relatively complex process and increased cost bring inconvenience to large-scale production.

5.4. Pulsed Lasers Based on TMDs

TMDs have occupied the important status in the potential candidates of SAs due to their large number of members.^[243] As another material that has been widely studied in the field of nonlinear optics after graphene, TMD is found to perform well in terms of switchable bandgap, higher third-order nonlinear optical response and ultrafast carrier dynamics. Taking MoS₂ for example, as the thickness decreases from bulk to a single layer, the bandgap of MoS₂ changes from indirect to direct, and the bandgap value increases from 1.29 to 1.8 eV.^[12] In addition, at 800 nm, MoS₂ shows a higher third-order nonlinear optical response than graphene.^[74] MoS₂ also represents ultrafast intraband relaxation time as short as 30 fs and carrier life-time nearly 100 ps.^[74]

At present, some TMD materials have made important breakthroughs in fiber lasers, the performance of MLFLs based on TMDs are provided in Table 7. As shown in Table 7, the pulse duration of the laser spans from tens of femtoseconds to several thousand picoseconds. In 2015, Zhang et al. not only characterized the ultra-wideband nonlinear absorption characteristics of layered MoS₂, but also successfully applied it to the YDFL, demonstrating its mode-locking ability.^[271] Zhang et al. implemented a broadband tunable ultrahigh speed MLFL using free-standing layered MoS₂–polymer composite. The tunable wavelength from 1535 to 1565 nm and the resulting picosecond pulses once again demonstrated the sub-bandgap absorption of MoS₂.^[260] Subsequently, the optical nonlinearity of WS₂ was

found by Wu et al. in EDFL.^[244] The resulting MDFL had a short pulse duration of 595 fs and SNR up to 75 dB, which indicated the potential of WS₂ in photonic applications. Mao et al. implemented WS₂-based MLFLs at 1.55 and 1.06 μm , respectively.^[246] They not only demonstrated the broadband saturable absorption characteristics of WS₂, but also calculated the bandgap of WS₂ nanosheets which in different defect states. Inspired by MoS₂ and WS₂, more and more TMDs are coming into vision. Mao et al. argued that MoSe₂ and WSe₂ theoretically have greater advantages in broadband absorption because of their smaller bandgaps, and further applied them to fiber lasers.^[278] Luo et al. observed the two-photon absorption phenomenon of MoSe₂ and investigated its effect on mode-locking operations. Based on MoSe₂ SA which with the MD of 0.63%, a stable MLFL with a pulse duration of 1.45 ps was obtained.^[280] Overall, the shortest pulse duration based on TMDs was achieved by Liu and his collaborators. They used a hybrid mode-locking of nonlinear polarization evolution and a WS₂ SA to obtain a pulse duration as low as 67 fs in Figure 15.^[249] Meanwhile, the 3 dB spectral width of up to 114 nm was also realized in the same work. The maximum fundamental frequency was obtained by Yan and his team, which was up to 396 MHz.^[253] However, the difference in PE is relatively large. Except for the lasers of up to 128.3 nJ implemented by the team of Yan et al.,^[252] the PE of another MLFLs varied from nJ to pJ.

Similarly, the summary of TMDs-based QSFLs achieved so far are shown in Table 8. Woodward et al. fabricated a few-layer MoS₂ SA by liquid-phase exfoliation, and applied it to a passively Q-switched YDFL, the pulse duration, repetition rate and PE of which were 2.88 μs , 74 kHz, and 126 nJ, respectively. Moreover, the central wavelength of the system was tunable in the range of 1030–1070 nm.^[314] Xia et al. also prepared MoS₂ films by a

Table 7. Performance summary of MLFLs based on TMDs.

Materials	MD [%]	Repetition frequency [MHz]	λ [nm]/ $\Delta\lambda$	Pulse duration [fs]	SNR [dB]	Mode locked threshold [mW]	Power [mW]	Maximum pulse energy [nJ]	Ref.
WS ₂	2.9	–	1572/5.2	595	75	260	–	–	[244]
	0.7	8.83	1560/11.48	605	50	–	10.1	1.14	[50]
	1.5	14.57	1556/3.2	820	47.1	–	20	0.00139	[245]
	5.1	8.05	1565/14.5	21100	–	85	1.8	2.2	[246]
	2.9	5.57	1063/0.77	630000	–	–	76	13.6	[246]
	3.53	19.57	1563.8/5.19	808	60.5	41	2.64	0.1336	[247]
	14.79	41.1	1560/19	288	58	–	18.4	–	[248]
	35.1	135	1540/114	67	93	–	–	–	[249]
	17.22	101.4	1561/57	246	92	–	18	–	[250]
	10.9	34.8	1941/5.6	1300	–	–	0.6	0.0172	[251]
	15.1	–	1568.3/1.94	1490	71.8	–	62.5	128.3	[252]
	4.48	396	150.1/26.1	1.03×10^6	56.3	30	4.75	–	[253]
	1.2	19.58	1559.7/6.6	675	65	54	0.625	–	[254]
	2.06	2.84	1030.3/1.1	2.5×10^6	48	87	8.02	2.82	[68]
	7.8	19.57	1560/6.75	395	64	65	1.5	0.0766	[75]
	4.48	352	1560/0.031	–	61	410	5.28	–	[75]
	8.5	4.2	1565.3/2.4	1360	–	30	37	8.8	[255]
	1.78	–	1034.2/1	2.4×10^6	–	140	–	2.82	[256]
	3	–	1572/5.2	595	75	260	–	–	[257]
	6	3.481	1562/1.1	2430	57	184	7	2.12	[258]
MoSe ₂	11	10.2	1557/4	660	65	14.4	–	–	[259]
	10.69	12.99	1552/3	960	–	–	–	0.065	[260]
	12.5	13.9	1926/2.86	1510	55	350	6	–	[261]
	11.3	13.2	1090/0.27	21840	29	–	20	1.48	[262]
	–	27.1	1573.7/7.3	630	61	25	3.82	0.141	[263]
	4	5.78	1567.7/2.3	1400	55	350	–	–	[264]
	3.6	26.5	1037/2.6	4.75×10^5	65	160	32	1.21	[265]
	16.1	0.987	1563/1.05	2170	71.4	–	–	–	[266]
	–	–	1565/12.8	1000	–	–	–	0.065	[267]
	–	216	1570/2.8	1420	60.2	44	6.81	–	[268]
	10.7	13	1535/1565	1070	–	–	–	–	[269]
	11	15.43	1037.5/0.9	1.55×10^6	40.5	125	1.5	0.097	[270]
	0.8	16.33	1558.35/2.9	1000	52	–	–	–	[271]
	9.3	–	1054.3/2.7	8×10^5	50	–	9.3	–	[272]
–	9.12	1979/2.1	1970	45	–	20	2.2	[273]	
WSe ₂	19.48	34.7	1563.4/13.6	256	75	40	63.8	2	[274]
	1.83	11.36	1863.96/3.19	1160	53	650	32.5	–	[275]
	52.38	58.5	1562/14	185	95	–	30	–	[276]
	–	11.357	1863.96/2.89	1260	85	–	–	–	[277]
	0.5	5.25	1557.6/2.1 1562.6/2.2	1250	–	35	0.84	–	[278]
MoSe ₂	21.89	63.127	1557.4/25.8	163.5	96	–	28.5	–	[279]
	5.4	15.38	1557.3/5.4	798	59.1	–	22.8	0.0067	[279]
	7.3	8.8	1560/7.8	580	50	65	–	0.0913	[71]
	0.63	–	1558.25/1.67	1450	61.5	–	0.443	0.0548	[280]
	4.4	18.21	1912/4.62	920	65	274	4.3	–	[281]
	4.98	23.53	1943.35/4.38	980	65	–	9.3	0.39	[282]
	0.8	16.27	1558.35/2.9	1000	52	30.7	–	–	[271]

Table 7. Continued.

Materials	MD [%]	Repetition frequency [MHz]	λ [nm]/ $\Delta\lambda$	Pulse duration [fs]	SNR [dB]	Mode locked threshold [mW]	Power [mW]	Maximum pulse energy [nJ]	Ref.
WTe ₂	4.2	15.38	1557.3/5.1	737	38.2	–	–	–	[283]
	22,57	64.56	1552/12.72	207	85	–	–	–	[284]
	25	18.72	1915.5/3.13	1250	95	580	39.9	2.13	[285]
	8.4	30	1973.4/4	2700	>60	158	1.17	–	[286]
MoTe ₂	2.85	13.98	1556.2/4.14	770	67	–	0.04	–	[287]
	1.46	–	1559.3/1.06	2460	62	–	0.12	–	[288]
	25.5	21.601	1559.57/11.76	229	93	–	57	2.14	[289]
TiS ₂	1.8	5.26	1561/2.4	1200	>50	–	–	–	[290]
	5.7	14.353	1930.22/4.45	952	87.8	–	36.7	2.56	[291]
	8.3	22.7	1563.3/4.75	800	>60	–	–	0.0253	[292]
	ReS ₂	1.896	–	1565/1	2549	65	–	12	0.037
–		14.53	–	270	–	–	1.08	–	[294]
1		3.4383	1563/2.6	1247	60	–	–	–	[125]
HfS ₂	0.25	1.78	1563.3/8.2	3800	68	410	–	–	[295]
	0.12	5.48	1558.6/	1600	–	–	0.4	–	[296]
	15.7	21.45	1561.8/12.2	221.7	70	30	89.4	4.17	[297]
	NbSe ₂	3.72	7.7	1566/2.45	756	50	15	–	–
3.155		12.3	1027/0.155	3.8×10^5	43	175	–	–	[298]
SnS ₂	0.76	39.27	1062.66/8.63	6.56×10^5	53	175	2.23	–	[299]
	4.6	29.27	1562.01/6.09	623	>45	125	1.2	–	[300]
	0.6	3.7596	1025/1.2	2.83×10^5	60	–	–	0.492	[301]
SnSe ₂	5	4.3976	1561/1.6	1630	60	–	–	27.2	[301]
	–	1.9876	1910/1.2	–	60	–	–	513	[301]
	20.67	15.03	1563.4/2.9	2.76×10^5	–	47	14.74	0.96	[302]

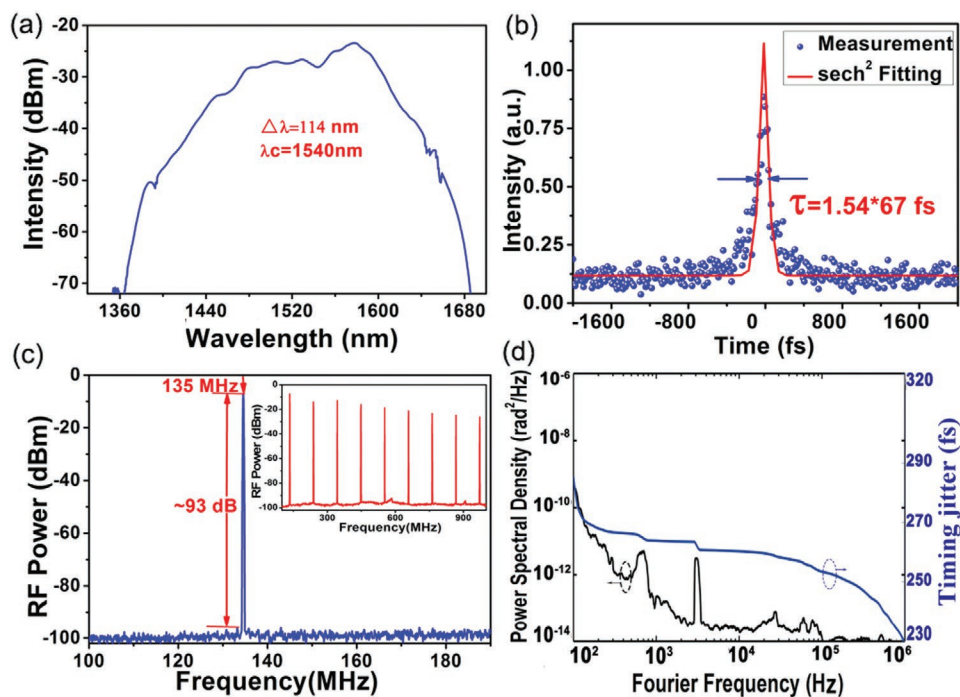


Figure 15. Performance of MLFL based on TMDs. a) The spectrum; b) intensity autocorrelation trace; c) RF spectrum; d) phase noise curve. Reproduced with permission. Reproduced with permission.^[249] Copyright 2017, The Optical Society.

Table 8. Performance summary of QSFLs based on TMDs.

Materials	MD [%]	Repetition frequency [kHz]	λ	Pulse duration [μ s]	SNR [dB]	Q-switching threshold [mW]	Power [mW]	Maximum pulse energy [nJ]	Ref.
WS ₂	3.12	24.9–36.7	1030	3.2–6.4	53	–	0.5	13.6	[303]
	4.85	79–97	1558	1.1–3.4	44	–	6.4	179.6	[303]
	10.17	36.78–81.75	–	1–3.61	–	50	<4.5	56.5	[304]
	4.1	7.7–35.2	1558–1559	2.6–19.3	43.1	12.7	4.1	0.12	[305]
	1.4	80–120	1547.5	0.958	–	290	4.66	44	[306]
	4.48	91–258	1560	0.16	40	50	17.3	54.4	[75]
	7.7	29.5–367.8	1560	0.1549–1.269	42	10	25.2	68.5	[307]
	2	16.15–60.88	1560	2.376	60	30	9.5	195	[308]
	2.9	90–125	1570	–	–	252	<6	46.3	[244]
	2.53	47.03–77.925	1560	3.966–6.707	54.2	400	8.07dB	1179.4	[309]
MoS ₂	20.9	27.17–101.17	–	1.4–3	–	40	<0.12	<1.2	[310]
	8.6	38.43	1550	5.02	37	57	5.43	141.3	[311]
	28.5	28.6–114.8	1560.5	1.92–3.7	41.1	42	<1	8.2	[312]
	4	72.74–86.39	1566.98	3.53–5.18	51.6	258	6.47	74.93	[264]
	–	22	1550–1575	6–35	40	–	150	–	[313]
	6.3	65.3–89	1055	2.68–4.4	45	–	9.36	126	[314]
	2.15	7.758–41.452	1560	9.92–13.528	48.5	50	1.16 dB	184.7	[315]
	7.7	25.27	1562	3.19	37.8	14.8	2.27	0.09	[316]
	11.07	92–212	1530.9	0.888	60	147	18.8	88	[122]
	1.6	6.4–28.9	1066.5	5.8	44.6	211.2	0.9	32.6	[317]
WSe ₂	1.6	6.5–27	1565	5.4–23.3	54.5	15.5	1.7	63.2	[317]
	1.6	27.6–48.1	2032	1.76	54.6	2.89 W	47.3	1000	[317]
	25.25	77–242	1562	1.2–4.3	72	118	26.7	110	[318]
	4.25	92.46–138	1560	0.754–1.478	50	170	4.25 dB	12–29	[319]
	3.5	4.5–49.6	1560	3.1–7.9	46.7	240	1.23	13.5–27.2	[320]
	3.02	46.281–85.365	1560	4.063–9.182	41.9	280	5dB	484.8	[309]
	16.82	80.32–204.2	1530	0.581	65	210	17.1	83.7	[321]
	25.69	64–122	1558	1.53–5.75	57	160	17.16	140.7	[325]
	1.2	28.5–90	1491–1502	1–2	35.97	110	<0.16	<2.5	[322]
	38	55.5–78.12	1036.69/1039.22	1.2–2.4	28	200	0.077	0.99	[323]
MoSe ₂	0.63	9.9	1558.25	13.6	–	10	–	–	[280]
	–	16.9–32.8	1562.3	30.4–59.1	–	22.4	1.9	57.9	[324]
	4.7	60–74.9	1060	2.8–4.6	–	–	8.72	116	[119]
	4.7	26.5–35.4	1566	4.8–7.9	–	–	18.9	825	[119]
	4.7	14–21.8	1924	5.5–16	–	–	0.13	42	[119]
	6.73	60.724–66.847	1560	4.04–6.506	25.3	570	3.9dB	369.5	[309]
	2.18	19–79	1044	1	–	110	2.2	28.3	[325]
	25.06	144.7–240	1525	0.583	55	212	14.07	58.625	[326]
	17.47	148–228	1559	0.677	63	225	25	109	[327]
	25.92	70–154	1530	1.13	62	192	<12	<75	[328]
TiSe ₂	25.92	70–154	1530	1.13	62	192	<12	<75	[328]
TiS ₂	8.3	25.2–50.7	1560.2	4–6.6	40.56–	–	9.5	–	[292]
SnSe ₂	10.6	74.1–168.7	1060	0.966–2.635	>40	243	18.03	106.9	[329]
SnS ₂	3.15	172.3–227	1532.7	0.51–1.01	50	290	9.27	<40	[330]
ReS ₂	0.12	12.6–19	1557.3	5.496–23	–	20	1.2	62.8	[296]
	–	43–64	1532	2.1–7.4	52.5	110	–2.48	38	[331]
ZrS ₂	3.3	16.37–76.92	1563	2.3–10	–	90	4.08	53	[332]
NbSe ₂	–	24.03–45.24	1527	2.53–5.12	52.5	42	4.44	98.19	[333]
ReSe ₂	–	6.64–21.04	1566	4.916.5	40.7	140	0.76	36	[334]

CVD method, and further a fiber-compatible MoS₂ SA was formed.^[312] Based on a linear cavity, stable Q-switched pulses were achieved at 1560.5 nm, the corresponding pulse duration obtained was 1.92 μs. By using fiber Bragg grating with different central wavelengths, the lasing wavelengths of Q-switching operations could be adjusted from 1529.8 to 1570.1 nm. Chen et al. demonstrated a WS₂-SAM with high-damage-resistant by magnetron sputtering technique.^[307] The shortest pulse duration of optical soliton which centered at 1560 nm was 15.94 ns. The AOP and PE were 25.2 mW and 68.5 nJ. The saturable absorption characteristics of WS₂ and corresponding WS₂-based QSFLs were explored by Zhang et al.^[303] Two QSFLs at 1030 and 1558 nm were achieved, the pulse duration and PE were 3.2 μs, 13.6 nJ and 1.3 μs, 179.6 nJ. Chen et al. reported 4 different SAs, such as MoS₂, WS₂, MoSe₂, and WSe₂ using the same preparation method, then compared their nonlinear characteristics and the performance of the corresponding QSFLs.^[309] Among them, MoSe₂-PVA exhibited the highest MD of 6.73%. WS₂-based QSFLs had highest extinction ratio and the best stability, meanwhile, the intracavity PE is highest which ranged from 822.9 to 1179.4 nJ. These studies provided a meaningful reference for the further targeted design of lasers. The PE of QSFL realized by Chen et al. was as high as 1179.4 nJ.^[309] Compared with the MLFLs, QSFLs can only achieve ns-order pulse duration, but the PE obtained by QSFLs is almost better than one or two orders of magnitude.

Although the bandgap of TMDs is mostly distributed in the range of 1–2 eV, the sub-band absorption (the photon energy is below the optical bandgap) has been widely observed in TMD-based lasers. Reliable studies have shown that the defect state may cause a reduction in the bandgap, which results in the sub-band absorption.^[280] In the theory of defect state, the imperfection of 2D material is inevitable in the production process, which has an impact on both its electronic and optical properties. Yu et al. has demonstrated that the MoS₂ bandgap can be reduced from 1.08 to 0.08 eV by introducing the defects in a suitable range.^[335] However, although this defect state makes TMDs applicable to infrared and mid-infrared photon devices, the defects introduced by general preparation methods are uncontrollable. If defects are to be controlled, it will inevitably make the preparation process more complicated. Moreover, this defect state will affect the quality of the material to some extent. Obviously, the wide bandgap makes the optical response of TMDs mainly concentrated in the visible light band.

5.5. Thickness-Dependent Photonic Devices

A variety of 2D materials have been successfully implemented in lasers as SA. However, because these 2D materials only show nanometer-scale gaps in thickness, researchers tend to focus on the variety of materials and neglect the property changes caused by the thickness differences of the same materials. More and more studies have shown that thickness plays an important role in the properties of materials.

Bao et al. found that by changing the thickness of graphene, the MD of which can be adjusted from 66.5% to 6.2%.^[4] Although BPs maintain a direct bandgap when the thickness changes, the band structure has an adjustable range from 0.3 eV (bulk

structure) to 1.5 eV (single layer), which greatly affects the applied band range.^[336,337] The effect of thickness on TMDs is even more pronounced. When the number of layers of these materials is gradually reduced to a few or even a single layer, due to the quantum confinement effect, the bandgap structure changes from indirect to direct, and the bandgap value will increase in a certain range, thus affecting the relaxation process of interband electrons and making the materials exhibit unique electrical and optical properties.^[338–341] In recent years, as the research heat of 2D materials has gradually warmed up, there are numerous research directions related to preparation processes, properties research, and applied research, but the problems of the relationship between size, thickness, and material properties are still unclear. Therefore, the investigation of the difference in the application of layer-regulated 2D photonic devices in lasers is an important scientific problem to be solved in the laser applications.

The MD, as the main characterization parameter of the nonlinear absorption of SA which is greatly affected by thickness, has a great impact on the performance of the laser. As early as 2015, Jeon et al. theoretically analyzed the influence of MD on the performance of the mode-locked laser.^[342] When the net cavity GVD of the laser is set as -0.2 ps^2 , the pulse duration shows a downward trend as the MD increased. Meanwhile, as the MD increases in a certain range, the spectral bandwidth broadens. In recent years, these theoretical inferences have been verified in experiments. Liu et al. investigated the difference in the application of 2D photonic devices with different thicknesses in lasers for the first time based on WSe₂.^[276] Under the same preparation conditions, WSe₂ SAs with thicknesses of 1.5, 5.7, and 11 exhibited MDs of 52.38%, 47.38%, and 34.41% as shown in **Figure 16**, respectively. The WSe₂ SAs with different thicknesses were applied to the EDFLs, and three stable MLFLs were successfully obtained. It is found that the laser based on 1.5 nm WSe₂ owns the shortest pulse duration of 185 fs. Further, with the increase of the material thickness and the decrease of MD, the pulse duration of the laser gradually broadened, which was consistent with the theoretical calculation mentioned above. By comparing the parameters of different lasers, they obtained the variation law of pulse duration and 2D material thickness, which provides an important reference for engineering ultrafast photonic devices according to requirements. In order to further validate the experimental results, comparative experiments based on other materials were also successfully implemented. The project teams of Liu further realized the application of SnS₂ with different thickness in lasers.^[343] Unlike WSe₂, the MD of SnS₂ increases with the increase of thickness. The 108.7 nm SnS₂ had the maximum MD of 40.53%. However, the trend of pulse duration with MD is consistent with the previous discussion. The laser based on the SnS₂ SA with the largest modulated saturable absorber had the smallest pulse duration of 132.9 fs. To summarize, the influence of the thickness of the material on its MD may be positive or reverse, but the trend that the pulse width decreases as the MD increases is always consistent.

5.6. 2D Materials Heterostructure Based Pulsed Lasers

Although several materials introduced above have made great progress in the field of nonlinear optics, it is undeniable that

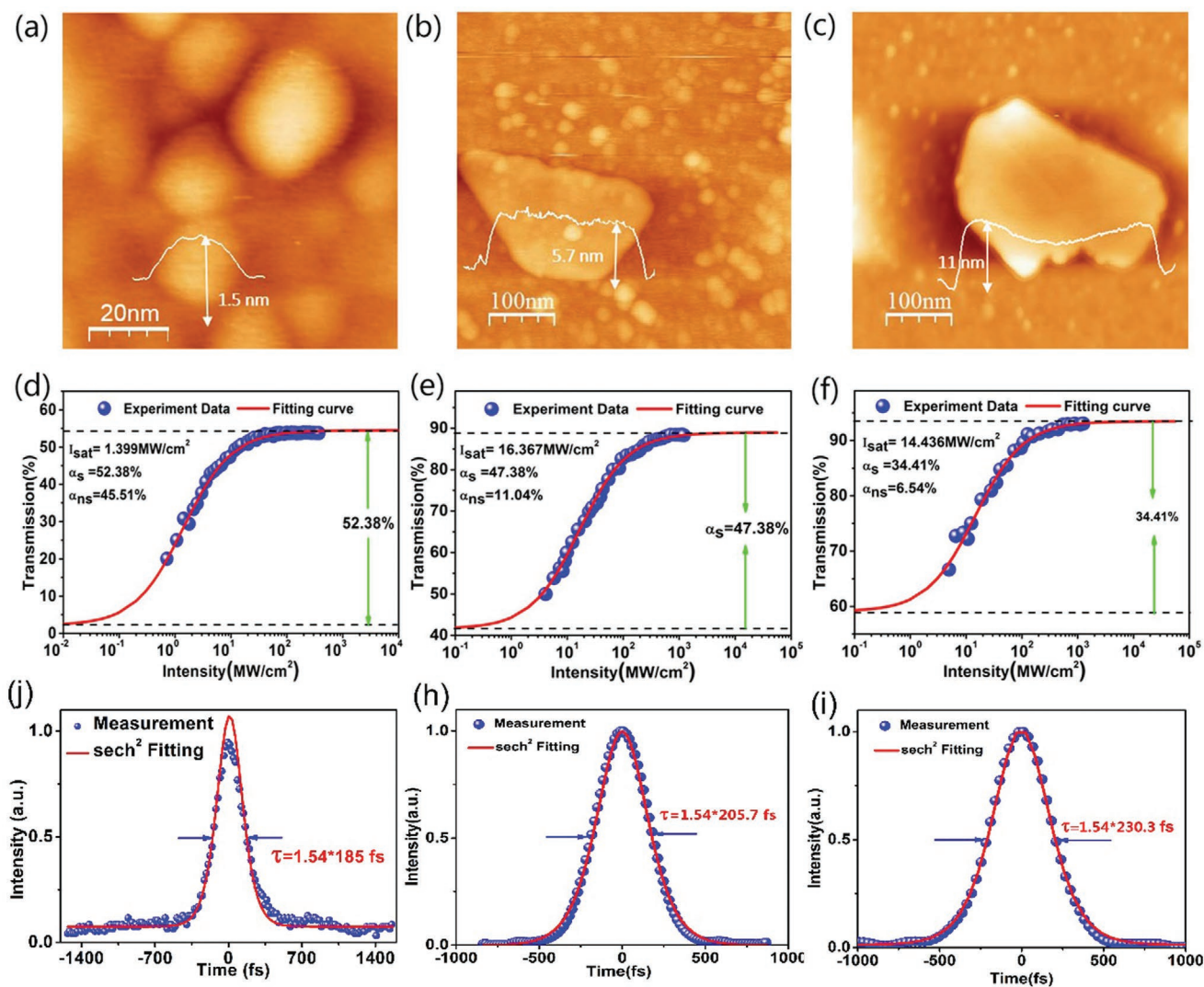


Figure 16. Performance of WSe₂ SA with different thickness. a–c) Morphology of WSe₂ measured with AFM. d–f) Power dependent nonlinear saturable absorption of the WSe₂ SA. h–j) The pulse duration of the WSe₂ SA. Reproduced with permission.^[276] Copyright 2018, The Royal Society of Chemistry.

each individual material often coexists with advantages and disadvantages. Because of their inherent nature, these disadvantages are inevitable, which may hinder their development to some extent. Inspired by the inspiration of “take advantage of one’s strengths and make up for one’s weaknesses,” people began to think about whether two or more materials can be compounded by a heterojunction structure, which can overcome the shortcomings of materials and at the same time superimpose the advantages of materials.

The summary of 2D materials heterostructure based MLFLs achieved so far are shown in **Table 9**.^[125,344–352] Graphene with Dirac cone structure and ultrafast recovery time has inherent advantages in broadband absorption and ultrashort pulse, but the optical MD of which is small.^[353,354] At the same time, TIs have been reported to have an MD of up to 70% at 1570 nm, but the long relaxation time more than 500 fs make them appear inferior to ultrafast photonics.^[105] To synthesize their advantages, Mu et al. successfully fabricated graphene-Bi₂Te₃ heterojunction for the first time and applied this heterojunction to

lasers.^[344] Bi₂Te₃ was grown directly on graphene by a two-step CVD method, which avoids the problem of lattice mismatch. At the same time, heterojunction products with different coverage were prepared by controlling the preparation conditions, and their nonlinear optical properties were measured separately. Experiments show that the heterojunction structure formed by the combination of graphene and Bi₂Te₃ not only makes up for the weakness of low MD of graphene, but also ensures the fast relaxation process of composites. More importantly, the saturated absorption, MD and electron relaxation time of graphene-Bi₂Te₃ heterojunction materials were adjustable. An MLFL based on graphene-Bi₂Te₃ was obtained, with a pulse duration of 837 fs and SNR of 60.7 dB as shown in **Figure 17**. The single PE was calculated to be 0.178 nJ. Similar graphene-TI heterojunctions were subsequently well applied in Yb-doped fiber lasers and wavelength-tunable lasers.^[345,346]

The successful application of this graphene-TI heterojunction has stimulated people’s interest in exploring new heterojunction materials. MoS₂/graphene nanocomposites

Table 9. Performance summary of MLFLs based on the 2D materials heterostructure.

Materials	MD [%]	Repetition frequency (MHz)	λ [nm]/ $\Delta\lambda$	Pulse duration [fs]	SNR [dB]	Mode-locked threshold [mW]	Power [mW]	Maximum pulse energy [nJ]	Ref.
Graphene–Bi ₂ Te ₃	15	17.3	1568/3.4	837	60.7	40	3.07	0.178	[344]
Graphene–Bi ₂ Te ₃	23.28	79.13	1058.9/3.5	189940	<50	75	2.53	0.032	[345]
Graphene–Bi ₂ Te ₃	18.98	6.91	1565.6/2.2	1170	67.4	30	–	–	[346]
	23.11	3.7	1049.1/4.3	144300	65	115	–	–	[346]
MoS ₂ /graphene	38.3	3.47	1571.8/1.5	2200	53.7	70	–	–	[347]
Graphene/MoS ₂	10.8	11.93	1571.8/3.5	830	60	24	5.85	0.49	[348]
Graphene/WS ₂	9.6	8.83	1568.3/2.3	1120	62	20	4.74	0.54	[349]
Graphene/ phosphorene	9	7.43	1529.92/3.4	820	52	–	–	–	[350]
	4.7	7.5	1525/19.4	148	58	–	–	–	[350]
MoS ₂ –Sb ₂ Te ₃ –MoS ₂	64.17	36.4	1554/28	286	>73	–	20	–	[124]
WS ₂ –MoS ₂ –WS ₂	16.99	36.46	1562.66/16.03	296	90.3	150	25	–	[351]
MoS ₂ –WS ₂	19.12	74.6	1560/24.4	154	91.2	–	19.8	–	[352]

which own exotic optical–electrical properties have attracted much attention. Experiments show that the covalent donor–acceptor structure formed by this complex mechanism enhances the saturable absorption of MoS₂/graphene nanocomposites. In addition, through Z-scan studies at different wavelengths, the broadband and enhanced saturable absorption of MoS₂/graphene nanocomposites were experimentally

found by Jiang et al.^[347] When MoS₂/graphene nanocomposites were applied into a laser, the mode-locked solitons with a pulse duration of 2.2 ps were successfully obtained, the SNR of which was up to 53.7 dB. The ultrashort pulses also have been realized by Liu et al. in an EDFL based on a MoS₂/graphene heterostructure SA. The soliton pulses were centered at 1571.8 nm with the pulse duration of 830 fs.^[348] Similarly, SA based on

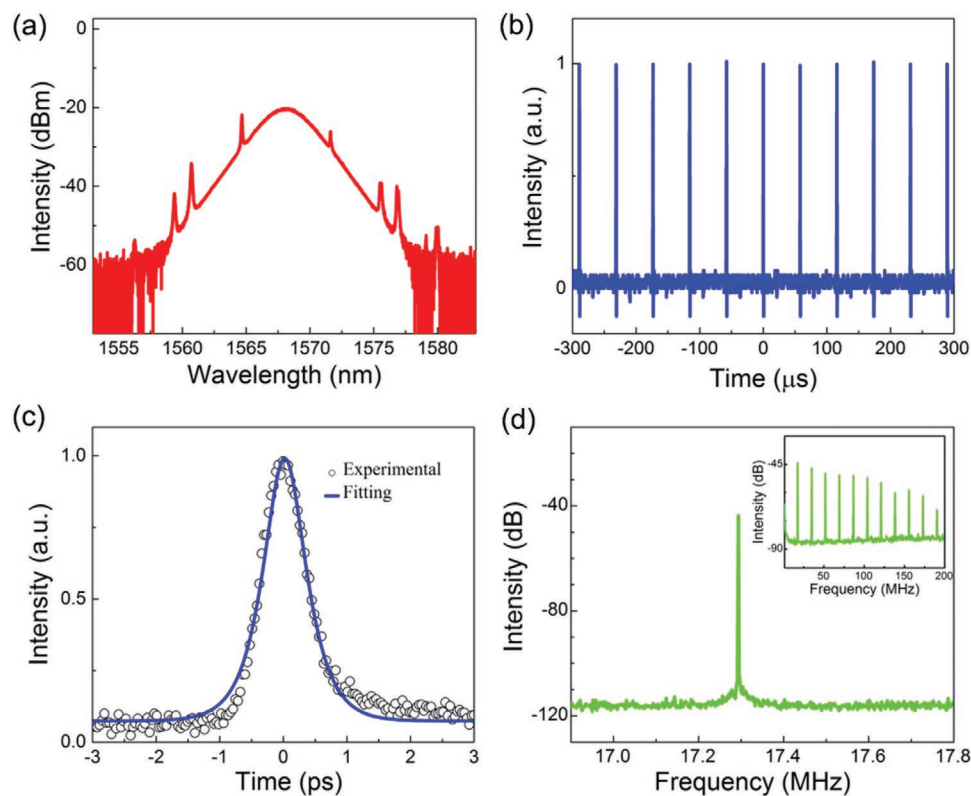


Figure 17. Performance of MLFL based on graphene–Bi₂Te₃ heterojunction. a) The spectrum; b) pulse train; c) intensity autocorrelation trace; d) RF spectrum. Reproduced with permission.^[344] Copyright 2015, American Chemical Society.

graphene/WS₂ heterostructure also performed well in optical nonlinearity. An MLFL based on graphene/WS₂ heterostructure has been established by Du et al.^[349] The resulting optical solitons which centered at 1568.3 nm with a 3 dB spectral width of 2.3 nm had a pulse duration of 1.12 ps.

As an important saturable absorber with direct bandgap, BP has attracted great interest because of its ultrafast carrier mobility. However, the unstable chemical properties make it indispensable for additional treatment in the application. The rise of heterogeneous structures provides new opportunities for solving this problem. Liu et al. put this idea into practice for the first time.^[350] By mixing graphene and BPs into heterostructures, the advantages of graphene and BPs are combined, it was reported that the performance of graphene-BP mixture is much better than individual graphene or BP. Moreover, the stability of heterostructures was improved compared to pristine BP. By adjusting the mixing ratio of graphene and BP, the nonlinear optical properties of the resulting heterojunction were able to be adjusted, which also provided a new train of thought for the development of new saturable absorbers. Furthermore, they have implemented an MLFL with prepared graphene-BP SA. The femtosecond MLFL operated at 1531 nm with a short pulse duration of 148 fs. Compared with the previous record based on BP, the pulse duration based on graphene-BP SA was reduced by $\approx 83\%$.^[215,221]

In view of the superiority of graphene materials, it has been frequently involved in the research of heterojunction materials, but the heterojunction materials based on nongraphene materials have also begun to attract increasing interest. TI, as a kind of saturable absorbing material with large MD and strong third-order nonlinearity, has always been of concern. TMD as the

most widely studied material after graphene, has been active in the field of optical nonlinearity, the high damage threshold makes it more advantageous in high power applications. To obtain ideal SA with both large MD and damage threshold, Liu et al. attempted to prepare MoS₂-Sb₂Te₃-MoS₂ heterojunction as a feasible method.^[124] By theoretical calculation, it is found that this heterojunction could effectively reduce the bandgap, which is conducive to broadband absorption of materials. Moreover, the damage threshold was greatly improved, almost 10 000 times that of commercially available SESAMs.^[307] Due to the strong nonlinearity of TI, the MoS₂-Sb₂Te₃-MoS₂ heterojunction exhibited a large MD up to 64%. The MLFL achieved by MoS₂-Sb₂Te₃-MoS₂ SA owned 3 dB bandwidth of 28 nm at 1554 nm as shown in **Figure 18**, the pulse duration and maximum AOP were 286 fs and 20 mW. This work provides an alternative to the preparation of high quality, highly controllable 2D materials.

Composites cannot only combine the advantages of different materials, but also magnify some advantages by the unexpected synergistic effect, leading to some attractive features or functions. This phenomenon has been observed and studied in TMD composites. Both MoS₂ and WS₂ are important members of TMDs and have wide and important applications in lasers as SA. It is worth mentioning that their mixture is even performed better than individual material. For example, a sub 50 fs hole time is observed in stacked MoS₂ and WS₂ heterostructures due to formed type II semiconductor heterojunctions.^[355] Compared with monolayer MoS₂ which with intralayer carrier recombination of 2 ps, the type II semiconductor heterojunction leads to two orders of magnitude reduction in photoelectrons transfer, making MoS₂-WS₂

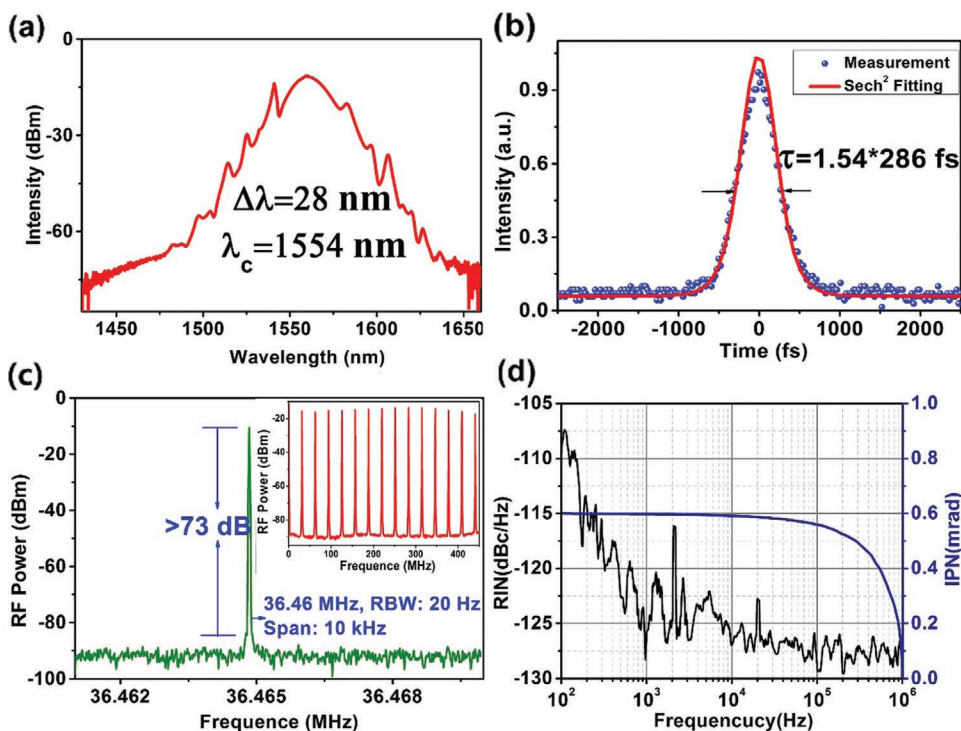


Figure 18. Performance of MLFL based on MoS₂-Sb₂Te₃-MoS₂ SA. a) The spectrum; b) intensity autocorrelation trace; c) RF spectrum; d) phase noise curve. Reproduced with permission. Reproduced with permission.^[125] Copyright 2017, Springer Nature.

composites more competitive in realizing ultrashort pulses. In addition, the absorption of the MoS₂-WS₂ heterostructure is superior to the simple superposition of the respective absorption of MoS₂ and WS₂,^[356] which effectively enhances the light-matter interaction. Chen et al. first demonstrated the remarkable nonlinear optical properties of WS₂-MoS₂-WS₂ heterostructure in EDFL. The pulse duration as short as 296 fs and average power as high as 25 mW further illustrated the superiority of WS₂-MoS₂-WS₂ heterostructure in optical nonlinearity.^[351] Soon afterward, Liu et al. combined heterojunction with tapered fiber to obtain a MoS₂-WS₂ SA with better performance.^[352] The MLFL based on prepared MoS₂-WS₂ SA owned the SNR of 91.2 dB and power jitter of 0.123, which indicated the remarkable stability of the system.

It is proved that the heterojunction material can overcome the shortcomings of materials and at the same time superimpose the advantages of materials, achieving a suitable equilibrium state. At the same time, the properties of the heterojunction can be controlled according to the proportion of each material, which indicates that the heterojunction structure has great potential in engineering design photonic devices.^[345] Therefore, heterojunction materials could be a strong candidate for future promising materials as SAs.

6. Conclusion and Outlook

In the past few years, from the basic research to the innovative technology development of next-generation, great leaps have been made in the research and application of ultrathin 2D nanomaterials in various fields. Undoubtedly, this tremendous advancement has thoroughly proved the unique role of dimensions in determining the intrinsic attributes of nanomaterials, and has paved the way for exploring its wider application. In this review, recent advances of 2D materials from the aspects of synthesis methods, characterization techniques, optical nonlinearity, and optical applications are categorized. Both bottom-up and top-down methods can be used to prepare ultrathin 2D nanomaterials, each with its own advantages and limitations. It is particularly noteworthy that structural features of ultrathin TMDs nanomaterials prepared by different synthetic methods, such as crystallinity, size, crystal phase, thickness, surface properties, defects, etc., are not in complete accord, therefore there are fields for their respective suitable applications. By means of appropriate characterization techniques, not only the structural information of the prepared material can be clearly displayed to the atomic level, but also the elemental composition, proportion and the corresponding valence state of the material can be accurately obtained, which is helpful for the research of their structure and properties as well as the correlation between them. The unique properties make them perform well in nonlinear optics, and may even replace existing commercial technologies while constantly exploring new applications and opportunities while they are constantly exploring new applications and opportunities.

The extensive application of 2D materials has injected new vitality into the laser field, but the larger and stricter application requirements have also brought new challenges to them. First of all, the existing mature preparation methods are difficult to

unite high quality and high yield. Recognized CVD methods that are capable of producing high-quality materials tend to require high operational complexity and cost, while methods for producing materials at large yields are difficult to guarantee high crystallinity and quality of materials. Considering the production speed, yield and quality, the preparation of 2D materials is not sufficient to meet the requirements of industry or commercialization. Therefore, how to achieve high-yield, high-quality, and cost-effective preparation methods to meet the needs of industrial and commercial applications is one of the major challenges currently facing. Accordingly, the characterization of the prepared materials is also one of the important areas to be improved. For ultrathin 2D materials, the understanding of the growth mechanism can be effectively fed back to the optimization of the preparation method, and the characterization of the basic properties provides an important basis and explanation for its subsequent application. Promisingly, Raman, XPS, SEM, and other technologies have provided tremendous help in exploring the characteristics of materials in recent years. However, how to conveniently and effectively observe the material growth process and quickly identify the material components, how to develop more powerful and easy-to-operate characterization techniques are still important challenges. Meanwhile, the relatively low physical and/or chemical stability of some 2D materials, does not endow them with long-term stability and durability, which makes them unsuitable for storage and the application of long-term stable optoelectronic devices. The sources of this instability are generally: 1) inevitable oxidation caused by direct exposure to air (for example, black phosphorus); 2) inevitable defects in the preparation process. Although there are some measures to increase the stability of 2D materials, such as coating and packaging, there are still large restrictions in the application. Therefore, how to find an economical and cost-effective way to ensure or extend the stability of materials in storage, processing, and application, and expand its application in long-term stability devices is another enormous challenge.

Although the current research on 2D materials is challenging, the opportunities that follow are also gratifying. In the future development of 2D materials, we think the following points are worthy of attention. 1) Continuous attempts and explorations of new materials cannot be stopped. The needs for SAs with ultra-broadband, ultrafast relaxation time, strong nonlinearity and high damage threshold are still urgent and persistent. 2) Changing material properties by doping. Doping can change the bandgap of the material or affect the electron relaxation process, thus changing the performance of 2D materials. 3) Improved the properties of 2D material through surface modification. This kind of research has begun to rise in recent years. For example, the environmental stability of BP was tried to enhance by attaching functional groups to the surface. 4) Phase modulation is also a feasible way to change the properties of 2D materials. Most 2D materials have different phases, and the performance of the same material with different phases is quite different.

Acknowledgements

The authors would like to thank the support from grants by the National Natural Science Foundation of China (NSFC) (11674036,

11875008, 61622406); Beijing Youth Top-Notch Talent Support Program (2017000026833ZK08); Fund of State Key Laboratory of Information Photonics and Optical Communications (Beijing University of Posts and Telecommunications, IPOC2017ZZ05); State Key Laboratory of Advanced Optical Communication Systems and Networks, Shanghai Jiao Tong University (2019GZKF03007); Beijing University of Posts and Telecommunications Excellent Ph.D. Students Foundation (CX2019202).

Conflict of Interest

The authors declare no conflict of interest.

Keywords

fiber lasers, nonlinear optical materials, saturable absorbers, thickness-dependent photonic devices, 2D materials

Received: September 28, 2019

Revised: December 10, 2019

Published online: February 20, 2020

-
- [1] R. P. Feynman, *Eng. Sci.* **1960**, 23, 22.
- [2] P. Ajayan, P. Kim, K. Banerjee, *Phys. Today* **2016**, 69, 38.
- [3] Y. F. Song, H. Zhang, L. M. Zhao, D. Y. Shen, D. Y. Tang, *Opt. Express* **2016**, 24, 1814.
- [4] Q. L. Bao, H. Zhang, Y. Wang, Z. H. Ni, Y. L. Yan, Z. X. Shen, K. P. Loh, D. Yuan, *Adv. Funct. Mater.* **2009**, 19, 3077.
- [5] Y. H. Xu, W. X. Wang, Y. Q. Ge, H. Y. Guo, X. J. Zhang, S. Chen, Y. H. Deng, Z. G. Lu, H. Zhang, *Adv. Funct. Mater.* **2017**, 27, 1702437.
- [6] Y. H. Xu, X. F. Jiang, Y. Q. Ge, Z. N. Guo, Z. K. Zeng, Q. H. Xu, H. Zhang, X. F. Yu, D. Y. Fan, *J. Mater. Chem. C* **2017**, 5, 3007.
- [7] Z. T. Wang, Y. H. Xu, S. C. Dhanabalan, J. Sophia, C. J. Zhao, C. W. Xu, Y. J. Xiang, J. Q. Li, H. Zhang, *IEEE Photonics J.* **2016**, 8, 1.
- [8] B. Guo, S. H. Wang, Z. X. Wu, Z. X. Wang, D. H. Wang, H. Huang, F. Zhang, Y. Q. Ge, H. Zhang, *Opt. Express* **2018**, 26, 22750.
- [9] X. T. Jiang, S. X. Liu, W. Y. Liang, S. J. Luo, Z. L. He, Y. Q. Ge, H. D. Wang, R. Cao, F. Zhang, Q. Wen, J. Q. Li, Q. L. Bao, D. Y. Fan, H. Zhang, *Laser Photonics Rev.* **2018**, 12, 1700229.
- [10] A. K. Geim, K. S. Novoselov, *Nat. Mater.* **2009**, 6, 11.
- [11] K. S. Novoselov, V. I. Fal'ko, L. Colombo, P. R. Gellert, M. G. Schwab, K. Kim, *Nature* **2012**, 490, 192.
- [12] S. Manzeli, D. Ovchinnikov, D. Pasquier, O. V. Yazyev, A. Kis, *Nat. Rev. Mater.* **2017**, 2, 170333.
- [13] F. N. Xia, T. Mueller, Y. M. Lin, A. Valdes-Garcia, P. Avouris, *Nat. Nanotechnol.* **2009**, 4, 839.
- [14] B. Radisavljevic, A. Radenovic, J. Brivio, V. Giacometti, A. Kis, *Nat. Nanotechnol.* **2011**, 6, 147.
- [15] Z. Y. Yin, H. Li, H. Li, L. Jiang, Y. M. Shi, Y. H. Sun, G. Lu, Q. Zhang, X. D. Chen, H. Zhang, *ACS Nano* **2012**, 6, 74.
- [16] C. L. Tan, X. Y. Qi, Z. D. Liu, F. Zhao, H. Li, X. Huang, L. Shi, B. Zheng, X. Zhang, L. H. Xie, Z. Y. Tang, W. Huang, H. Zhang, *J. Am. Chem. Soc.* **2015**, 137, 1565.
- [17] C. L. Tan, Z. D. Liu, W. Huang, H. Zhang, *Chem. Soc. Rev.* **2015**, 44, 2615.
- [18] L. K. Li, Y. J. Yu, G. J. Ye, Q. Q. Ge, X. D. Ou, H. Wu, D. L. Feng, X. H. Chen, Y. B. Zhang, *Nat. Nanotechnol.* **2014**, 9, 372.
- [19] T. Li, E. Cinquanta, D. Chiappe, C. Grazianetti, M. Fanciulli, M. Dubey, A. Molle, D. Akinwande, *Int. J. Nanotechnol.* **2013**, 10, 22.
- [20] X. H. Chen, G. H. Xu, X. H. Ren, Z. J. Li, X. Qi, K. Huang, H. Zhang, Z. Y. Huang, J. X. Zhong, *J. Mater. Chem. A* **2017**, 5, 6581.
- [21] Z. N. Guo, S. Chen, Z. Z. Wang, Z. Y. Yang, F. Liu, Y. H. Xu, J. H. Wang, Y. Yi, H. Zhang, L. Liao, P. K. Chu, X. F. Yu, *Adv. Mater.* **2017**, 29, 1703811.
- [22] Z. Y. Huang, W. J. Han, H. L. Tang, L. Ren, D. S. Chander, X. Qi, H. Zhang, *2D Mater.* **2015**, 2, 035011.
- [23] Q. Y. He, S. X. Wu, Z. Y. Yin, H. Zhang, *Chem. Sci.* **2012**, 3, 1764.
- [24] A. N. Abbas, B. L. Liu, L. Chen, Y. Q. Ma, S. Cong, N. Aroonyadet, M. Köp, T. Nilges, C. W. Zhou, *ACS Nano* **2015**, 9, 5618.
- [25] H. Y. Guo, C. Y. Lan, Z. F. Zhou, P. H. Sun, D. P. Wei, C. Li, *Nanoscale* **2017**, 9, 6246.
- [26] G. Y. Lee, S. Y. Kim, S. W. Jung, S. W. Jang, J. H. Kim, *Sens. Actuators, B* **2017**, 250, 569.
- [27] T. Dinh, H. P. Phan, D. V. Dao, P. Woodfield, A. Qamara, N. T. Nguyen, *J. Mater. Chem. C* **2015**, 3, 8776.
- [28] S. M. Feng, Z. Lin, X. Gan, R. T. Lv, M. Terrones, *Nanoscale Horiz.* **2017**, 2, 72.
- [29] M. Y. Tsai, A. Tarasov, Z. R. Hesabi, H. Taghinejad, P. M. Campbell, C. A. Joiner, A. Adibi, E. M. Vogel, *ACS Appl. Mater. Interfaces* **2015**, 7, 12850.
- [30] T. Wang, Y. L. Guo, P. B. Wan, X. M. Sun, H. Zhang, Z. Z. Yu, X. D. Chen, *Nanoscale* **2017**, 9, 869.
- [31] G. Lalwani, A. M. Henslee, B. Farshid, L. J. Lin, F. K. Kasper, Y. X. Qin, A. G. Mikos, B. Sitharaman, *Biomacromolecules* **2013**, 14, 900.
- [32] K. Yang, L. Z. Feng, X. Z. Shi, Z. Liu, *Chem. Soc. Rev.* **2013**, 42, 530.
- [33] L. Cheng, J. J. Liu, X. Gu, H. Gong, X. Z. Shi, T. Liu, C. Wang, X. Y. Wang, G. Liu, H. Y. Xing, W. B. Bu, B. Q. Sun, Z. Liu, *Adv. Mater.* **2014**, 26, 1886.
- [34] Y. Chen, C. L. Tan, H. Zhang, L. Z. Wang, *Chem. Soc. Rev.* **2015**, 44, 2681.
- [35] X. D. Zhang, X. Xie, H. Wang, J. J. Zhang, B. C. Pan, Y. Xie, *J. Am. Chem. Soc.* **2013**, 135, 18.
- [36] M. Chen, S. H. Tang, Z. D. Guo, X. Y. Wang, S. G. Mo, X. Q. Huang, G. Liu, N. F. Zheng, *Adv. Mater.* **2014**, 26, 8210.
- [37] Y. Chen, D. L. Ye, M. Y. Wu, H. R. Chen, L. L. Zhang, J. L. Shi, L. Z. Wang, *Adv. Mater.* **2014**, 26, 7019.
- [38] T. J. Fan, Y. S. Zhou, M. Qiu, H. Zhang, *J. Innovative Opt. Health Sci.* **2018**, 11, 1830003.
- [39] Z. B. Sun, Y. T. Zhao, Z. B. Li, H. D. Cui, Y. Y. Zhou, W. H. Li, W. Tao, H. Zhang, H. Y. Wang, P. K. Chu, X. F. Yu, *Small* **2017**, 13, 1602896.
- [40] F. Yin, K. Hu, S. Chen, D. Y. Wang, J. N. Zhang, M. S. Xie, D. Yang, M. Qiu, H. Zhang, Z. G. Li, *J. Mater. Chem. B* **2017**, 5, 5433.
- [41] M. Qiu, D. Wang, W. Y. Liang, L. P. Liu, Y. Zhang, X. Chen, D. K. Sang, C. Y. Xing, Z. J. Li, B. Q. Dong, F. Xing, D. Y. Fan, S. Y. Bao, H. Zhang, Y. H. Cao, *Proc. Natl. Acad. Sci. USA* **2018**, 115, 501.
- [42] W. Tao, X. Y. Ji, X. D. Xu, M. A. Islam, Z. J. Li, S. Chen, P. E. Saw, H. Zhang, Z. Bharwani, Z. L. Guo, J. J. Shi, O. C. Farokhzad, *Angew. Chem., Int. Ed.* **2017**, 56, 11896.
- [43] Z. P. Sun, T. Hasan, F. Torrisi, D. Popa, G. Privitera, F. Q. Wang, F. Bonaccorso, D. M. Basko, A. C. Ferrari, *ACS Nano* **2010**, 4, 803.
- [44] H. J. Zhang, C. X. Liu, X. L. Qi, X. Dai, Z. Fang, S. C. Zhang, *Nat. Phys.* **2009**, 5, 438.
- [45] K. C. Park, J. S. Lee, Y. T. Lee, W. K. Choi, J. H. Lee, Y. W. Song, *Ann. Phys.* **2015**, 527, 770.
- [46] P. G. Yan, R. Y. Lin, S. C. Ruan, A. J. Liu, H. Chen, *Opt. Express* **2015**, 23, 154.
- [47] H. Liu, X. W. Zheng, M. Liu, N. Zhao, A. P. Luo, Z. C. Luo, W. C. Xu, H. Zhang, C. J. Zhao, S. C. Wen, *Opt. Express* **2014**, 22, 6868.
- [48] K. Wu, C. S. Guo, H. Wang, X. Y. Zhang, J. Wang, J. P. Chen, *Opt. Express* **2017**, 25, 17639.
- [49] H. D. Xia, H. P. Li, C. Y. Lan, C. Li, X. X. Zhang, S. J. Zhang, Y. Liu, *Opt. Express* **2014**, 22, 17341.

- [50] B. Guo, Y. Yao, P. G. Yan, K. Xu, J. J. Liu, S. G. Wang, Y. Li, *IEEE Photonics Technol. Lett.* **2016**, *28*, 323.
- [51] S. Q. Chen, L. L. Miao, X. Chen, Y. Chen, C. J. Zhao, S. Datta, Y. Li, Q. L. Bao, H. Zhang, Y. Liu, S. C. Wen, D. Y. Fan, *Adv. Opt. Mater.* **2015**, *3*, 1769.
- [52] Y. Zhou, M. X. Zhang, Z. N. Guo, L. L. Miao, S. T. Han, Z. Y. Wang, X. W. Zhang, H. Zhang, Z. C. Peng, *Mater. Horiz.* **2017**, *4*, 997.
- [53] J. L. Zheng, Z. H. Yang, C. Si, Z. M. Liang, X. Chen, R. Cao, Z. N. Guo, K. Wang, Y. Zhang, J. H. Ji, M. Zhang, D. Y. Fan, H. Zhang, *ACS Photonics* **2017**, *4*, 1466.
- [54] G. P. Zheng, Y. Chen, H. H. Huang, C. J. Zhao, S. B. Lu, S. Q. Chen, H. Zhang, S. C. Wen, *ACS Appl. Mater. Interfaces* **2013**, *5*, 10288.
- [55] H. Zhang, D. Y. Tang, L. M. Zhao, Q. L. Bao, K. P. Loh, *Opt. Commun.* **2010**, *283*, 3334.
- [56] J. Du, M. Zhang, Z. Guo, J. Chen, X. Zhu, G. Hu, P. Peng, Z. Zheng, H. Zhang, *Sci. Rep.* **2017**, *7*, 42357.
- [57] P. F. Li, Y. Chen, T. S. Yang, Z. Y. Wang, H. Lin, Y. H. Xu, L. Li, H. R. Mu, B. N. Shivananju, Y. P. Zhang, Q. L. Zhang, A. L. Pan, S. J. Li, D. Y. Tang, B. H. Jia, H. Zhang, Q. L. Bao, *ACS Appl. Mater. Interfaces* **2017**, *9*, 12759.
- [58] L. Lu, X. Tang, R. Cao, L. M. Wu, Z. J. Li, G. H. Jing, B. Q. Dong, S. B. Lu, Y. Li, Y. J. Xiang, J. Q. Li, D. Y. Fan, H. Zhang, *Adv. Opt. Mater.* **2017**, *5*, 1700301.
- [59] Q. K. Wang, Y. Chen, L. L. Miao, G. B. Jiang, S. Q. Chen, J. Liu, X. Q. Fu, C. J. Zhao, H. Zhang, *Opt. Express* **2015**, *23*, 7681.
- [60] L. M. Wu, Z. J. Xie, L. Lu, J. L. Zhao, Y. Z. Wang, X. T. Jiang, Y. Q. Ge, F. Zhang, S. B. Lu, Z. N. Guo, J. Liu, Y. J. Xiang, S. X. Xu, J. Q. Li, D. Y. Fan, H. Zhang, *Adv. Opt. Mater.* **2018**, *6*, 1700985.
- [61] L. M. Wu, X. T. Jiang, J. L. Zhao, W. Y. Liang, Z. J. Li, W. C. Huang, Z. T. Lin, Y. Z. Wang, F. Zhang, S. B. Lu, Y. J. Xiang, S. X. Xu, J. Q. Li, H. Zhang, *Laser Photonics Rev.* **2018**, *12*, 1800215.
- [62] L. M. Wu, Y. Z. Dong, J. L. Zhao, D. T. Ma, W. C. Huang, Y. Zhang, Y. Z. Wang, X. T. Jiang, Y. J. Xiang, J. Q. Li, Y. Q. Feng, J. L. Xu, H. Zhang, *Adv. Mater.* **2019**, *31*, 1807981.
- [63] K. S. Novoselov, A. K. Geim, S. V. Morozov, D. Jiang, Y. Zhang, S. V. Dubonos, I. V. Grigorieva, A. A. Firsov, *Science* **2004**, *306*, 666.
- [64] D. J. Late, *ACS Appl. Mater. Interfaces* **2014**, *6*, 15881.
- [65] B. K. Miremedi, S. R. Morrison, *J. Catal.* **1987**, *103*, 334.
- [66] K. S. Novoselov, D. Jiang, F. Schedin, T. J. Booth, V. V. Khotkevich, S. V. Morozov, A. K. Geim, *Proc. Natl. Acad. Sci. USA* **2005**, *102*, 10451.
- [67] S. W. Wang, Y. Zhou, Y. Wang, S. Yan, Y. Li, W. G. Zheng, Y. Deng, Q. H. Zhu, J. Q. Xu, Y. L. Tang, *Laser Phys. Lett.* **2016**, *13*, 055102.
- [68] H. Y. Guoyu, Y. R. Song, K. X. Li, Z. Y. Dou, J. R. Tian, X. P. Zhang, *Laser Phys. Lett.* **2015**, *12*, 125102.
- [69] Z. Tian, K. Wu, L. C. Kong, N. Yang, Y. Wang, R. Chen, W. S. Hu, J. Q. Xu, Y. L. Tang, *Laser Phys. Lett.* **2015**, *12*, 065104.
- [70] L. Li, Y. G. Wang, H. Sun, L. N. Duan, X. Wang, J. H. Si, *Opt. Eng.* **2015**, *54*, 046101.
- [71] H. B. Ahmad, S. N. Aidit, N. A. Hassan, M. F. Ismail, Z. C. Tiu, *Opt. Eng.* **2016**, *55*, 076115.
- [72] Z. Q. Luo, Y. Z. Huang, J. Weng, H. H. Cheng, Z. Q. Lin, B. Xu, Z. P. Cai, H. Y. Xu, *Opt. Express* **2013**, *21*, 29516.
- [73] Y. Z. Huang, Z. Q. Luo, Y. Y. Li, M. Zhong, B. Xu, K. J. Che, H. Y. Xu, Z. P. Cai, J. Peng, J. Weng, *Opt. Express* **2014**, *22*, 25258.
- [74] K. P. Wang, J. Wang, J. T. Fan, M. Lotya, A. O'Neill, D. Fox, Y. Y. Feng, X. Y. Zhang, B. X. Jiang, Q. Z. Zhao, H. Z. Zhang, J. N. Coleman, L. Zhang, W. J. Blau, *ACS Nano* **2013**, *7*, 9260.
- [75] H. Chen, L. Li, S. C. Ruan, T. Guo, P. G. Yan, *Opt. Eng.* **2016**, *55*, 081318.
- [76] S. M. Eichfeld, L. Hossain, Y. C. Lin, A. F. Piasecki, B. Kupp, A. G. Birdwell, R. A. Burke, N. Lu, X. Peng, J. Li, A. Azcatl, S. McDonnell, R. M. Wallace, M. J. Kim, T. S. Mayer, J. M. Redwing, J. A. Robinson, *ACS Nano* **2015**, *9*, 2080.
- [77] Z. Y. Zeng, Z. Y. Yin, X. Huang, H. Li, Q. Y. He, G. Lu, F. Boey, H. Zhang, *Angew. Chem., Int. Ed.* **2011**, *50*, 11093.
- [78] K. Fukuda, K. Akatsuka, Y. Ebina, R. Z. Ma, K. Takada, I. Nakai, T. Sasaki, *ACS Nano* **2008**, *2*, 1689.
- [79] M. Osada, G. Takanashi, B. W. Li, K. Akatsuka, Y. Ebina, K. Ono, H. Funakubo, K. Takada, T. Sasaki, *Adv. Funct. Mater.* **2011**, *21*, 3482.
- [80] M. S. Dresselhaus, A. Jorio, R. Saito, *Annu. Rev. Condens. Matter Phys.* **2010**, *1*, 89.
- [81] M. Velický, M. A. Bissett, C. R. Woods, P. S. Toth, T. Georgiou, I. A. Kinloch, K. S. Novoselov, R. A. W. Dryfe, *Nano Lett.* **2016**, *16*, 2023.
- [82] H. Li, J. Wu, Z. Y. Yin, H. Zhang, *Acc. Chem. Res.* **2014**, *47*, 1067.
- [83] Y. H. Lee, X. Q. Zhang, W. J. Zhang, M. T. Chang, C. T. Lin, K. D. Chang, Y. C. Yu, J. T. W. Wang, C. S. Chang, L. J. Li, T. W. Lin, *Adv. Mater.* **2012**, *24*, 2320.
- [84] A. V. Crewe, *J. Microsc.* **1974**, *100*, 247.
- [85] A. S. George, Z. Mutlu, R. Ionescu, R. J. Wu, J. S. Jeong, H. H. Bay, Y. Chai, K. A. Mkhoyan, M. Ozkan, C. S. Ozkan, *Adv. Funct. Mater.* **2014**, *24*, 7461.
- [86] M. Y. Li, Y. M. Shi, C. C. Cheng, L. S. Lu, Y. C. Lin, H. L. Tang, M. L. Tsai, C. W. Chu, K. H. Wei, J. H. He, W. H. Chang, K. Suenaga, L. J. Li, *Science* **2015**, *349*, 524.
- [87] Y. Y. Peng, Z. Y. Meng, C. Zhong, J. Lu, W. C. Yu, Y. B. Jia, Y. T. Qian, *Chem. Lett.* **2001**, *30*, 772.
- [88] X. P. Fang, X. Q. Yu, S. F. Liao, Y. F. Shi, Y. S. Hu, Z. X. Wang, G. D. Stucky, L. Q. Chen, *Microporous Mesoporous Mater.* **2012**, *151*, 418.
- [89] J. M. Hollander, W. L. Jolly, *Acc. Chem. Res.* **1970**, *3*, 193.
- [90] M. A. Baker, R. Gilmore, C. Lenardi, W. Gissler, *Appl. Surf. Sci.* **1999**, *150*, 255.
- [91] S. H. Su, Y. T. Hsu, Y. H. Chang, M. H. Chiu, C. L. Hsu, W. T. Hsu, W. H. Chang, J. H. He, L. J. Li, *Small* **2014**, *10*, 2589.
- [92] G. Eda, H. Yamaguchi, D. Voiry, T. Fujita, M. W. Chen, M. Chhowalla, *Nano Lett.* **2011**, *11*, 5111.
- [93] D. J. Late, B. Liu, H. S. S. Ramakrishna Matte, C. N. R. Rao, V. P. Dravid, *Adv. Funct. Mater.* **2012**, *22*, 1894.
- [94] C. G. Lee, H. G. Yan, L. E. Brus, T. F. Heinz, J. Hone, S. M. Ryu, *ACS Nano* **2010**, *4*, 2695.
- [95] S. Zhang, J. Yang, R. J. Xu, F. Wang, W. F. Li, M. Ghufuran, Y. W. Zhang, Z. F. Yu, G. Zhang, Q. H. Qin, Y. R. Lu, *ACS Nano* **2014**, *8*, 9590.
- [96] P. Tonndorf, R. Schmidt, P. Böttger, X. Zhang, J. Börner, A. Liebig, M. Albrecht, C. Kloc, O. Gordan, D. R. T. Zahn, S. M. de Vasconcellos, R. Bratschitsch, *Opt. Express* **2013**, *21*, 4908.
- [97] D. Li, R. B. Kaner, *Science* **2008**, *320*, 1170.
- [98] J. L. Zheng, X. Tang, Z. H. Yang, Z. M. Liang, Y. X. Chen, K. Wang, Y. F. Song, Y. Zhang, J. H. Ji, Y. Liu, D. Y. Fan, H. Zhang, *Adv. Opt. Mater.* **2017**, *5*, 1700026.
- [99] M. Z. Hasan, C. L. Kane, *Rev. Mod. Phys.* **2010**, *82*, 3045.
- [100] K. H. Nam, J. H. Choi, C. M. Park, *J. Electrochem. Soc.* **2017**, *164*, A2056.
- [101] G. Cunningham, D. Hanlon, N. McEvoy, G. S. Duesberg, J. N. Coleman, *Nanoscale* **2015**, *7*, 198.
- [102] R. R. Nair, P. Blake, A. N. Grigorenko, K. S. Novoselov, T. J. Booth, T. Stauber, N. M. R. Peres, A. K. Geim, *Science* **2008**, *320*, 1308.
- [103] K. F. Mak, L. Ju, F. Wang, T. F. Heinz, *Solid State Commun.* **2012**, *152*, 1341.
- [104] S. B. Lu, C. J. Zhao, Y. H. Zou, S. Q. Chen, Y. Chen, Y. Li, H. Zhang, S. C. Wen, D. Y. Tang, *Opt. Express* **2013**, *21*, 2072.
- [105] S. Q. Chen, C. J. Zhao, Y. Li, H. H. Huang, S. B. Lu, H. Zhang, S. C. Wen, *Opt. Mater. Express* **2014**, *4*, 587.
- [106] H. Zhang, X. He, W. Lin, R. F. Wei, F. T. Zhang, X. Du, G. P. Dong, J. R. Qiu, *Opt. Express* **2015**, *23*, 13376.

- [107] G. Z. Wang, S. F. Zhang, X. Y. Zhang, L. Zhang, Y. Cheng, D. Fox, H. Z. Zhang, J. N. Coleman, W. J. Blau, J. Wang, *Photonics Res.* **2015**, *3*, A51.
- [108] A. G. Čabo, J. A. Miwa, S. S. Grønberg, J. M. Riley, J. C. Johannsen, C. Cacho, O. Alexander, R. T. Chapman, E. Springate, M. Grioni, J. V. Lauritsen, D. C. King, P. Hofmann, S. Ulstrup, *Nano Lett.* **2015**, *15*, 5883.
- [109] J. H. Sun, Y. J. Gu, D. Y. Lei, S. P. Lau, W. T. Wong, K. Y. Wong, H. L. W. Chan, *ACS Photonics* **2016**, *3*, 2434.
- [110] P. Steinleitner, P. Merkl, P. Nagler, J. Mornhinweg, C. Schüller, T. Korn, A. Chernikov, R. Huber, *Nano Lett.* **2017**, *17*, 1455.
- [111] J. D. Zhang, X. F. Yu, W. J. Han, B. Lv, X. H. Li, S. Xiao, Y. L. Gao, J. He, *Opt. Lett.* **2016**, *41*, 1704.
- [112] Y. R. Shen, *The Principles of Nonlinear Optics*, Wiley-Interscience, New York, **1984**.
- [113] R. W. Boyd, *Nonlinear Optics*, Academic Press, New York, **2007**.
- [114] R. N. Zitter, *Appl. Phys. Lett.* **1969**, *14*, 73.
- [115] X. Zheng, Y. W. Zhang, R. Z. Chen, X. A. Cheng, Z. J. Xu, T. Jiang, *Opt. Express* **2015**, *23*, 15616.
- [116] X. Zheng, R. Z. Chen, G. Shi, J. W. Zhang, Z. J. Xu, X. A. Cheng, T. Jiang, *Opt. Express* **2015**, *40*, 3480.
- [117] D. H. Liu, B. Gu, B. X. Ren, C. G. Lu, J. He, Q. W. Zhan, Y. P. Cui, *J. Appl. Phys.* **2016**, *119*, 073103.
- [118] W. J. Liu, M. L. Liu, Y. Y. Ouyang, H. R. Hou, G. L. Ma, M. Lei, Z. Y. Wei, *Nanotechnology* **2018**, *29*, 174002.
- [119] R. I. Woodward, R. C. T. Howe, T. H. Runcorn, G. Hu, F. Torrisi, E. J. R. Kelleher, T. Hasan, *Opt. Express* **2015**, *23*, 20051.
- [120] X. D. Liu, S. L. Guo, H. T. Wang, L. T. Hou, *Opt. Commun.* **2001**, *197*, 431.
- [121] N. N. Dong, Y. X. Li, S. F. Zhang, N. McEvoy, X. Y. Zhang, Y. Cui, L. Zhang, G. S. Duesberg, J. Wang, *Opt. Lett.* **2016**, *41*, 3936.
- [122] M. L. Liu, Y. Y. Ouyang, H. R. Hou, M. Lei, W. J. Liu, Z. Y. Wei, *Chin. Phys. B* **2018**, *27*, 084211.
- [123] Y. H. Lin, C. Y. Yang, J. H. Liou, C. P. Yu, G. R. Lin, *Opt. Express* **2013**, *21*, 16763.
- [124] W. J. Liu, Y. N. Zhu, M. L. Liu, B. Wen, S. B. Fang, H. Teng, M. Lei, L. M. Liu, Z. Y. Wei, *Photonics Res.* **2018**, *6*, 220.
- [125] Y. D. Cui, F. F. Lu, X. M. Liu, *Sci. Rep.* **2017**, *7*, 40080.
- [126] Y. Li, Y. L. He, Y. Cai, S. Q. Chen, J. Liu, Y. Chen, X. Yuanjiang, *Laser Phys. Lett.* **2018**, *15*, 025301.
- [127] H. Yu, X. Chen, H. Zhang, X. Xu, X. Hu, Z. Wang, J. Wang, S. Zhuang, M. Jiang, *ACS Nano* **2010**, *4*, 7582.
- [128] Q. Bao, H. Zhang, Z. Ni, Y. Wang, L. Polavarapu, Z. Shen, Q. Xu, D. Tang, K. P. Loh, *Nano Res.* **2011**, *4*, 297.
- [129] J. H. Los, K. V. Zakharченко, M. I. Katsnelson, A. Fasolino, *Phys. Rev. B* **2015**, *91*, 045415.
- [130] M. Zhang, E. J. R. Kelleher, F. Torrisi, Z. Sun, T. Hasan, D. Popa, F. Wang, A. C. Ferrari, S. V. Popov, J. R. Taylor, *Opt. Express* **2012**, *20*, 25077.
- [131] P. L. Huang, S. C. Lin, C. Y. Yeh, H. H. Kuo, S. H. Huang, G. R. Lin, L. J. Li, C. Y. Su, W. H. Cheng, *Opt. Express* **2012**, *20*, 2460.
- [132] A. Martinez, K. Fuse, S. Yamashita, *Appl. Phys. Lett.* **2011**, *99*, 121107.
- [133] G. Sobon, J. Sotor, K. M. Abramski, *Laser Phys. Lett.* **2012**, *9*, 581.
- [134] G. Sobon, J. Sotor, I. Pasternak, A. Krajewska, W. Strupinski, K. M. Abramski, *Opt. Express* **2013**, *21*, 12797.
- [135] X. Y. He, Z. B. Liu, D. N. Wang, *Opt. Lett.* **2012**, *37*, 2394.
- [136] G. Sobon, J. Sotor, K. M. Abramski, *Appl. Phys. Lett.* **2012**, *100*, 161109.
- [137] G. W. Zhu, X. S. Zhu, F. Q. Wang, S. Xu, Y. Li, X. L. Guo, K. Balakrishnan, R. A. Norwood, N. Peyghambarian, *IEEE Photonics Technol. Lett.* **2015**, *28*, 7.
- [138] Q. Q. Wang, T. Chen, B. Zhang, M. Li, Y. Lu, K. P. Chen, *Appl. Phys. Lett.* **2013**, *102*, 131117.
- [139] B. Fu, Y. Hua, X. S. Xiao, H. W. Zhu, Z. P. Sun, C. X. Yang, *IEEE J. Sel. Top. Quantum Electron.* **2014**, *20*, 411.
- [140] G. Sobon, *Photonics Res.* **2015**, *3*, A56.
- [141] N. H. Park, H. Jeong, S. Y. Choi, M. H. Kim, F. Rotermund, D. Yeom, *Opt. Express* **2015**, *23*, 19806.
- [142] J. Sotor, I. Pasternak, A. Krajewska, W. Strupinski, G. Sobon, *Opt. Express* **2015**, *23*, 27503.
- [143] M. Pawliszewska, T. Martynkien, A. Przewłoka, J. Sotor, *Opt. Lett.* **2018**, *43*, 38.
- [144] H. Zhang, D. Tang, R. J. Knize, L. Zhao, Q. L. Bao, K. P. Loh, *Appl. Phys. Lett.* **2010**, *96*, 111112.
- [145] Z. P. Sun, D. Popa, T. Hasan, F. Torrisi, F. Q. Wang, E. J. R. Kelleher, J. C. Travers, V. Nicolosi, A. C. Ferrari, *Nano Res.* **2010**, *3*, 653.
- [146] Z. Q. Luo, M. Zhou, J. Weng, G. M. Huang, H. Y. Xu, C. C. Ye, Z. P. Cai, *Opt. Lett.* **2010**, *35*, 3709.
- [147] D. Popa, Z. P. Sun, T. Hasan, F. Q. Wang, A. C. Ferrari, *Appl. Phys. Lett.* **2011**, *98*, 073106.
- [148] W. J. Cao, H. Y. Wang, A. P. Luo, Z. C. Luo, W. C. Xu, *Laser Phys. Lett.* **2012**, *9*, 54.
- [149] J. Liu, S. D. Wu, Q. H. Yang, P. Wang, *Opt. Lett.* **2011**, *36*, 4008.
- [150] Z. T. Wang, Y. Chen, C. J. Zhao, H. Zhang, S. C. Wen, *IEEE Photonics J.* **2012**, *4*, 869.
- [151] J. Liu, J. Xu, P. Wang, *Opt. Commun.* **2012**, *285*, 5319.
- [152] Y. K. Yap, R. M. De La Rue, C. H. Pua, S. W. Harun, H. Ahmad, *Chin. Opt. Lett.* **2012**, *10*, 041405.
- [153] G. Sobon, J. Sotor, J. Jagiello, R. Kozinski, K. Librant, M. Zdrojek, K. M. Abramski, *Appl. Phys. Lett.* **2012**, *101*, 241106.
- [154] L. Wei, D. P. Zhou, H. Y. Fan, W. K. Liu, *IEEE Photonics Technol. Lett.* **2011**, *24*, 309.
- [155] F. Wang, F. Torrisi, Z. Jiang, D. Popa, T. Hasan, Z. Sun, W. B. Cho, A. C. Ferrari, in *2012 Conf. on Lasers and Electro-Optics (CLEO)*, IEEE, **2012**, https://doi.org/10.1364/CLEO_AT.2012.JW2A.72; see also ref. [147].
- [156] Z. H. Wang, Z. Wang, Y. G. Liu, R. J. He, G. D. Wang, G. Yang, S. M. Han, *Laser Phys. Lett.* **2018**, *15*, 055101.
- [157] Y. Y. Ren, M. Feng, A. B. Ren, K. Zhang, J. Yang, G. Q. Sun, T. H. Wang, Z. Y. Li, Y. G. Li, Z. B. Liu, *Laser Phys.* **2019**, *29*, 085101.
- [158] E. G. Mishchenko, *Phys. Rev. Lett.* **2009**, *103*, 24680.
- [159] C. Wei, X. Zhu, F. Wang, Y. Xu, K. Balakrishnan, F. Song, R. A. Norwood, N. Peyghambarian, *Opt. Lett.* **2013**, *38*, 3233.
- [160] I. H. Baek, H. W. Lee, S. Bae, B. H. Hong, Y. H. Ahn, D. Yeom, F. Rotermund, *Appl. Phys. Express* **2012**, *5*, 032701.
- [161] Y. Ando, *J. Phys. Soc. Jpn.* **2013**, *82*, 102001.
- [162] F. Bernard, H. Zhang, S. P. Gorza, P. Emplit, presented at *Advanced Photonics Congress 2012: Proc. of Nonlinear Photonics*, Colorado Springs, Colorado USA, June **2012**, paper NTh1A.5.
- [163] Y. H. Lin, S. F. Lin, Y. C. Chi, C. L. Wu, C. H. Cheng, W. H. Tseng, G. R. Lin, *ACS Photonics* **2015**, *2*, 481.
- [164] C. Zhao, H. Zhang, X. Qi, Y. Chen, Z. Wang, S. Wen, D. Tang, *Appl. Phys. Lett.* **2012**, *101*, 211106.
- [165] C. Chi, J. Lee, J. Koo, J. H. Lee, *Laser Phys.* **2014**, *24*, 105106.
- [166] J. Lee, J. Koo, Y. M. Jhon, J. H. Lee, *Opt. Express* **2014**, *22*, 6165.
- [167] M. Jung, J. Lee, J. Koo, J. Park, Y. W. Song, K. Lee, S. Lee, J. H. Lee, *Opt. Express* **2014**, *22*, 7865.
- [168] P. G. Yan, R. Y. Lin, H. Chen, H. Zhang, A. J. Liu, H. P. Yang, S. C. Ruan, *IEEE Photonics Technol. Lett.* **2014**, *27*, 264.
- [169] K. Yin, B. Zhang, L. Li, T. Jiang, X. F. Zhou, J. Hou, *Photonics Res.* **2015**, *3*, 72.
- [170] D. Mao, B. Q. Jiang, X. T. Gan, C. J. Ma, Y. Chen, C. J. Zhao, H. Zhang, J. B. Zheng, J. L. Zhao, *Photonics Res.* **2015**, *3*, A43.
- [171] L. N. Duan, Y. G. Wang, C. W. Xu, L. Li, Y. S. Wang, *IEEE Photonics J.* **2015**, *7*, 1.
- [172] K. Yin, T. Jiang, X. Zheng, H. Yu, X. G. Cheng, J. Hou, preprint, arXiv:1505.06322, **2015**; see also ref. [169].
- [173] Y. H. Lin, C. Y. Yang, S. F. Lin, W. H. Tseng, Q. L. Bao, C. I. Wu, G. R. Lin, *Laser Phys. Lett.* **2014**, *11*, 055107.

- [174] J. H. Lin, G. H. Huang, C. H. Ou, K. C. Che, W. R. Liu, S. Y. Tasy, Y. H. Chen, *IEEE Photonics J.* **2018**, *10*, 1502410.
- [175] H. Haris, H. Arof, A. R. Muhammad, C. L. Anyi, S. J. Tan, N. Kasim, S. W. Harun, *Opt. Fiber Technol.* **2019**, *48*, 117.
- [176] X. L. Han, H. N. Zhang, C. Zhang, C. H. Li, Q. X. Guo, J. J. Gao, S. Z. Jiang, B. Y. Man, *Appl. Opt.* **2019**, *58*, 2695.
- [177] N. N. Xu, H. N. Zhang, B. Y. Man, *Appl. Opt.* **2018**, *57*, 8811.
- [178] B. Guo, Y. Yao, Y. F. Yang, Y. J. Yuan, R. L. Wang, S. G. Wang, B. Yan, *J. Appl. Phys.* **2015**, *117*, 063108.
- [179] K. X. Li, Y. R. Song, Z. H. Yu, R. Q. Xu, Z. Y. Dou, J. R. Tian, *Laser Phys. Lett.* **2015**, *12*, 105103.
- [180] B. Guo, Y. Yao, J. J. Xiao, R. L. Wang, J. Y. Zhang, *IEEE J. Sel. Top. Quantum Electron.* **2015**, *22*, 8.
- [181] Y. C. Meng, G. Semaan, M. Salhi, A. Niang, K. Guesmi, Z. C. Luo, F. Sanchez, *Opt. Express* **2015**, *23*, 23053.
- [182] C. J. Zhao, Y. H. Zou, Y. Chen, Z. T. Wang, S. B. Lu, H. Zhang, S. C. Wen, D. Y. Tang, *Opt. Express* **2012**, *20*, 27888.
- [183] Z. Y. Dou, Y. R. Song, J. R. Tian, J. H. Liu, Z. H. Yu, X. H. Fang, *Opt. Express* **2014**, *22*, 24055.
- [184] J. Lee, J. H. Lee, *Chin. Phys. B* **2018**, *27*, 094219.
- [185] J. Sotor, G. Sobon, K. M. Abramski, *Opt. Express* **2014**, *22*, 13244.
- [186] J. Sotor, G. Sobon, K. Grodecki, K. M. Abramski, *Appl. Phys. Lett.* **2014**, *104*, 251112.
- [187] J. Boguslawski, J. Sotor, G. Sobon, J. Tarka, J. Jagiello, W. Macherzynski, L. Lipinska, K. M. Abramski, *Laser Phys.* **2014**, *24*, 105111.
- [188] J. Sotor, G. Sobon, W. Macherzynski, P. Paletko, K. Grodecki, K. M. Abramski, *Opt. Mater. Express* **2014**, *4*, 1.
- [189] Z. H. Wang, C. Y. Li, J. W. Ye, Z. Wang, Y. G. Liu, *Laser Phys. Lett.* **2019**, *16*, 025103.
- [190] J. T. Wang, J. D. Yin, T. C. He, P. G. Yan, *Chin. Phys. B* **2018**, *27*, 084214.
- [191] M. Kowalczyk, J. Boguslawski, R. Zybala, K. Mars, A. Mikula, G. Soboń, J. Sotor, *Opt. Mater. Express* **2016**, *6*, 2273.
- [192] J. Sotor, G. Sobon, J. Boguslawski, J. Tarka, K. M. Abramski, in *Fiber Lasers XII: Technology, Systems, and Applications*, Vol. 9344 (Eds: L. B. Shaw, J. Ballato), International Society for Optics and Photonics, San Francisco, CA, USA **2015**, p. 93441Z.
- [193] J. Tarka, J. Boguslawski, R. Zybala, M. Kowalczyk, G. Sobon, J. Sotor, in *Fiber Lasers XIII: Technology, Systems, and Applications*, Vol. 9728 (Ed: J. Ballato), International Society for Optics and Photonics, San Francisco, CA, USA **2016**, p. 972820.
- [194] W. J. Liu, L. H. Pang, H. N. Han, W. L. Tian, H. Chen, M. Lei, P. G. Yan, Z. Y. Wei, *Sci. Rep.* **2016**, *6*, 19997.
- [195] J. Lee, J. Koo, C. Chi, J. H. Lee, *J. Opt.* **2014**, *16*, 085203.
- [196] J. Lee, M. Jung, J. Koo, C. Chi, J. H. Lee, *IEEE J. Sel. Top. Quantum Electron.* **2014**, *21*, 31.
- [197] K. Yan, J. Lin, Y. Zhou, C. Gu, L. X. Xu, *Appl. Opt.* **2016**, *55*, 3026.
- [198] J. Koo, J. Lee, C. Chi, J. H. Lee, *J. Opt. Soc. Am. B* **2014**, *31*, 2157.
- [199] X. F. Rong, S. Y. Luo, W. S. Li, S. S. Jiang, X. G. Yan, X. F. Guan, Z. Y. Zhou, B. Xu, N. Chen, D. G. Wang, H. Y. Xu, Z. P. Cai, *Chin. Opt. Lett.* **2018**, *16*, 020016.
- [200] N. N. Xu, N. Ming, X. L. Han, B. Y. Man, H. N. Zhang, *Opt. Mater. Express* **2019**, *9*, 373.
- [201] W. W. Li, J. H. Zou, Y. Z. Huang, K. J. Wang, T. J. Du, S. S. Jiang, Z. Q. Luo, *Photonics Res.* **2018**, *6*, C29.
- [202] J. J. Zhang, D. D. Wu, C. J. Quan, Z. R. Guo, R. W. Zhao, R. P. Wang, S. X. Dai, Q. H. Nie, *J. Opt.* **2019**, *21*, 8.
- [203] N. Xu, H. Zhang, W. Yang, X. Han, B. Man, *Laser Phys.* **2018**, *28*, 125801.
- [204] H. Ahmad, M. A. M. Salim, S. R. Azzuhri, M. R. K. Soltanian, S. W. Harun, *Laser Phys.* **2015**, *25*, 065102.
- [205] H. Ahmad, M. R. K. Soltanian, L. Narimani, I. S. Amiri, A. Khodaei, S. W. Harun, *IEEE Photonics J.* **2015**, *7*, 1502508.
- [206] H. Haris, S. W. Harun, A. R. Muhammad, C. L. Anyi, S. J. Tan, F. Ahmad, R. M. Nor, N. R. Zulkepely, H. Arof, *Opt. Laser Technol.* **2017**, *88*, 121.
- [207] M. Q. Lokman, F. Ahmad, S. W. Harun, *EDP Sci.* **2017**, *162*, 010111.
- [208] J. Boguslawski, G. J. Soboń, K. Tarnowski, R. Zybala, K. Mars, A. Mikula, K. M. Abramski, J. Z. Sotor, *Opt. Eng.* **2016**, *55*, 081316.
- [209] P. G. Yan, H. Chen, K. Y. Li, C. Y. Guo, S. C. Ruan, J. Z. Wang, J. F. Ding, X. J. Zhang, T. Guo, *IEEE Photonics J.* **2015**, *8*, 1500506.
- [210] X. Ling, H. Wang, S. X. Huang, F. N. Xia, M. S. Dresselhaus, *Proc. Natl. Acad. Sci. USA* **2015**, *112*, 4523.
- [211] R. Zhang, Y. Zhang, H. Yu, H. Zhang, R. Yang, B. Yang, Z. Liu, J. Wang, *Adv. Opt. Mater.* **2015**, *3*, 1787.
- [212] K. Wang, B. M. Szydłowska, G. Wang, X. Zhang, J. J. Wang, J. J. Magan, L. Zhang, J. N. Coleman, J. Wang, W. J. Blau, *ACS Nano* **2016**, *10*, 6923.
- [213] Y. Chen, G. B. Jiang, S. Q. Chen, Z. N. Guo, X. F. Yu, C. J. Zhao, H. Zhang, Q. L. Bao, S. C. Wen, D. Y. Tang, D. Y. Fan, *Opt. Express* **2015**, *23*, 12823.
- [214] Z. C. Luo, M. Liu, Z. N. Guo, X. F. Jiang, A. P. Luo, C. J. Zhao, X. F. Yu, W. C. Xu, H. Zhang, *Opt. Express* **2015**, *23*, 20030.
- [215] J. Sotor, G. Sobon, W. Macherzynski, P. Paletko, K. M. Abramski, *Appl. Phys. Lett.* **2015**, *107*, 051108.
- [216] M. B. Hisyam, M. F. M. Rusdi, A. A. Latiff, S. W. Harun, *IEEE J. Sel. Top. Quantum Electron.* **2016**, *23*, 39.
- [217] D. Li, H. Jussila, L. Karvonen, G. Ye, H. Lipsanen, X. Chen, Z. P. Sun, *Sci. Rep.* **2015**, *5*, 15899.
- [218] K. Park, J. Lee, Y. T. Lee, W. K. Choi, J. H. Lee, Y. W. Song, *Ann. Phys.* **2015**, *527*, 770.
- [219] Y. F. Song, S. Chen, Q. Zhang, L. Li, L. M. Zhao, H. Zhang, D. Y. Tang, *Opt. Express* **2016**, *24*, 25933.
- [220] H. Yu, X. Zheng, K. Yin, X. A. Cheng, T. Jiang, *Appl. Opt.* **2015**, *54*, 10290.
- [221] Y. Chen, S. Q. Chen, J. Liu, Y. X. Gao, W. J. Zhang, *Opt. Express* **2016**, *24*, 13316.
- [222] M. H. M. Ahmed, A. A. Latiff, H. Arof, S. W. Harun, *Laser Phys. Lett.* **2016**, *13*, 095104.
- [223] D. Lee, K. Park, P. C. Debnath, I. Kim, Y. W. Song, *Nanotechnology* **2016**, *27*, 365203.
- [224] M. Pawliszewska, Y. Q. Ge, Z. J. Li, H. Zhang, J. Sotor, *Opt. Express* **2017**, *25*, 16916.
- [225] X. X. Jin, G. H. Hu, M. Zhang, Y. W. Hu, T. Albrow-Owen, R. C. T. Howe, T. C. Wu, Q. Wu, Z. Zheng, T. Hasan, *Opt. Express* **2018**, *26*, 12506.
- [226] H. Q. Song, Q. Wang, Y. F. Zhang, L. Li, *Opt. Commun.* **2017**, *394*, 157.
- [227] Y. Chen, H. Mu, P. F. Li, S. H. Lin, S. B. Nanjunda, Q. L. Bao, *Opt. Eng.* **2016**, *55*, 081317.
- [228] Y. Hu, X. Jin, G. Hu, M. Zhang, Q. Wu, Z. Zheng, T. Hasan, in *2018 Conf. on Lasers and Electro-Optics (CLEO)*, IEEE **2018**, p. 18024556; see also ref. [225].
- [229] J. Sotor, G. Sobon, M. Kowalczyk, W. Macherzynski, P. Paletko, K. M. Abramski, *Opt. Lett.* **2015**, *40*, 3885.
- [230] H. Mu, S. H. Lin, Z. C. Wang, S. Xiao, P. F. Li, Y. Chen, H. Zhang, H. F. Bao, S. P. Lau, C. X. Pan, D. Y. Fan, Q. L. Bao, *Adv. Opt. Mater.* **2015**, *3*, 1447.
- [231] H. Yu, X. Zheng, K. Yin, X. A. Cheng, T. Jiang, *Opt. Mater. Express* **2016**, *6*, 603.
- [232] F. A. A. Rashid, S. R. Azzuhri, M. A. M. Salim, R. A. Shaharuddin, M. A. Ismail, M. F. Ismail, M. Z. A. Razak, H. Ahmad, *Laser Phys. Lett.* **2016**, *13*, 085102.
- [233] T. Jiang, K. Yin, X. Zheng, H. Yu, X. A. Cheng, preprint, arXiv:1504.07341, **2015**; see also ref. [231].
- [234] H. Ahmad, M. A. M. Salim, K. Thambiratnam, S. F. Norizan, S. W. Harun, *Laser Phys. Lett.* **2016**, *13*, 095103.

- [235] A. H. H. Al-Masoodi, M. H. M. Ahmed, A. A. Latiff, H. Arof, S. W. Harun, *Chin. Phys. Lett.* **2016**, *33*, 054206.
- [236] Y. Z. Wang, J. F. Li, L. Han, R. G. Lu, Y. X. Hu, Z. Li, Y. Liu, *Laser Phys.* **2016**, *26*, 065104.
- [237] T. X. Feng, D. Mao, X. Q. Cui, M. K. Li, K. Song, B. Q. Jiang, H. Lu, W. M. Quan, *Materials* **2016**, *9*, 917.
- [238] J. L. Wang, Y. P. Xing, L. Chen, S. Li, H. T. Jia, J. F. Zhu, Z. Y. Wei, *J. Lightwave Technol.* **2018**, *36*, 2010.
- [239] T. Wang, X. X. Jin, H. S. Wu, J. X. Song, J. Wu, P. Zhou, in *2018 Asia Communications and Photonics Conf. (ACP)*, IEEE, **2018**, p. 18355920; see also ref. [240].
- [240] T. Wang, J. Wu, H. S. Wu, J. Wang, L. J. Huang, P. Zhou, *Opt. Laser Technol.* **2019**, *119*, 105618.
- [241] H. Q. Song, Q. Wang, D. D. Wang, L. Li, *Results Phys.* **2018**, *8*, 276.
- [242] J. O. Island, G. A. Steele, H. S. J. van der Zant, A. Castellanos-Gomez, *2D Mater.* **2015**, *2*, 011002.
- [243] Y. Zhang, H. Yu, R. Zhang, G. Zhao, H. Zhang, Y. Chen, L. Mei, M. Tonelli, J. Wang, *Opt. Lett.* **2017**, *42*, 547.
- [244] K. Wu, X. Y. Zhang, J. Wang, X. Li, J. P. Chen, *Opt. Express* **2015**, *23*, 11453.
- [245] J. Lee, J. Park, J. Koo, Y. M. Jhon, J. H. Lee, *J. Opt.* **2016**, *18*, 035502.
- [246] D. Mao, S. L. Zhang, Y. D. Wang, X. T. Gan, W. D. Zhang, T. Mei, Y. G. Wang, Y. S. Wang, H. B. Zeng, J. L. Zhao, *Opt. Express* **2015**, *23*, 27509.
- [247] P. G. Yan, A. J. Liu, Y. S. Chen, J. Z. Wang, S. C. Ruan, H. Chen, J. F. Ding, *Sci. Rep.* **2015**, *5*, 12587.
- [248] M. L. Liu, W. J. Liu, L. H. Pang, H. Teng, S. B. Fang, Z. Y. Wei, *Opt. Commun.* **2018**, *406*, 72.
- [249] W. J. Liu, L. H. Pang, H. N. Han, M. L. Liu, M. Lei, S. B. Fang, H. Teng, Z. Y. Wei, *Opt. Express* **2017**, *25*, 2950.
- [250] W. J. Liu, L. H. Pang, H. N. Han, K. Bi, M. Lei, Z. Y. Wei, *Nanoscale* **2017**, *9*, 5806.
- [251] M. W. Jung, J. S. Lee, J. Park, J. Koo, Y. M. Jhon, J. H. Lee, *Opt. Express* **2015**, *23*, 19996.
- [252] P. G. Yan, H. Chen, J. D. Yin, Z. H. Xu, J. R. Li, Z. K. Jiang, W. F. Zhang, J. Z. Wang, I. L. Li, Z. P. Sun, S. C. Ruan, *Nanoscale* **2017**, *9*, 1871.
- [253] P. G. Yan, H. Chen, A. J. Liu, K. Y. Li, S. C. Ruan, J. F. Ding, X. H. Qiu, T. Guo, *IEEE J. Sel. Top. Quantum Electron.* **2017**, *23*, 33.
- [254] P. G. Yan, A. J. Liu, Y. S. Chen, H. Chen, S. C. Ruan, C. Y. Guo, S. F. Chen, I. L. Li, H. P. Yang, J. G. Hu, G. Z. Cao, *Opt. Mater. Express* **2015**, *5*, 479.
- [255] Z. H. Wang, Z. Wang, Y. G. Liu, R. J. He, S. M. Han, G. D. Wang, G. Yang, X. Q. Wang, *Laser Phys. Lett.* **2018**, *15*, 085103.
- [256] H. Y. Guoyu, K. X. Li, Z. K. Dong, R. Q. Xu, J. R. Tian, Y. R. Song, presented at *Fifth Int. Symp. on Laser Interaction with Matter*, International Society for Optics and Photonics, China, March **2019**.
- [257] K. Wu, X. Y. Zhang, J. Wang, X. Li, J. P. Chen, *Science and Innovations*, Optical Society of America, CA, **2015**.
- [258] N. A. A. Kadir, E. I. Ismail, A. A. Latiff, H. Ahmad, H. Arof, S. W. Harun, *Chin. Phys. Lett.* **2017**, *34*, 014202.
- [259] L. Li, Y. L. Su, Y. G. Wang, X. Wang, Y. S. Wang, X. H. Li, D. Mao, J. H. Si, *IEEE J. Sel. Top. Quantum Electron.* **2017**, *23*, 44.
- [260] M. Zhang, R. C. T. Howe, R. I. Woodward, E. J. R. Kelleher, F. Torrisi, G. H. Hu, S. V. Popov, J. Roy Taylor, T. Hasan, *Nano Res.* **2015**, *8*, 1522.
- [261] L. M. Cao, X. Li, R. Zhang, D. D. Wu, S. X. Dai, J. Peng, J. Weng, Q. H. Nie, *Opt. Fiber Technol.* **2018**, *41*, 187.
- [262] M. F. M. Rusdi, A. A. Latiff, E. Hanafi, M. B. H. Mahyuddin, H. Shamsudin, K. Dimiyati, S. W. Harun, *Chin. Phys. Lett.* **2016**, *33*, 114201.
- [263] M. H. M. Ahmed, A. A. Latiff, H. Arof, H. Ahmad, S. W. Harun, *Opt. Laser Technol.* **2016**, *82*, 145.
- [264] Z. C. Luo, F. Z. Wang, H. Liu, M. Liu, R. Tang, A. P. Luo, W. C. X., *Opt. Eng.* **2016**, *55*, 081308.
- [265] Y. Zhang, J. Q. Zhu, P. X. Li, X. X. Wang, H. Yu, K. Xiao, C. Y. Li, G. Y. Zhang, *Opt. Commun.* **2018**, *413*, 236.
- [266] Z. K. Jiang, J. R. Li, H. Chen, J. Z. Wang, W. F. Zhang, P. G. Yan, *Opt. Commun.* **2018**, *406*, 44.
- [267] R. C. T. Howe, R. I. Woodward, G. H. Hu, Z. Y. Yang, E. J. R. Kelleher, T. Hasan, *Phys. Status Solidi B* **2016**, *253*, 911.
- [268] H. D. Xia, H. P. Li, C. Y. Lan, C. Li, G. L. Deng, J. F. Li, Y. Liu, *Chin. Phys. B* **2015**, *24*, 084206.
- [269] R. I. Woodward, R. C. T. Howe, G. Hu, F. Torrisi, M. Zhang, T. Hasan, E. J. R. Kelleher, *Photonics Res.* **2015**, *3*, A30.
- [270] S. Sathiyam, V. Velmurugan, K. Senthilnathan, P. Ramesh Babu, S. Sivabalan, *Laser Phys.* **2016**, *26*, 055103.
- [271] R. L. Zhang, J. Wang, X. Y. Zhang, J. T. Lin, X. Li, P. W. Kuan, Y. Zho, M. S. Liao, W. Q. Gao, *Chin. Phys. B* **2019**, *28*, 014207.
- [272] H. Zhang, S. B. Lu, J. Zheng, J. Du, S. C. Wen, D. Y. Tang, K. P. Loh, *Opt. Express* **2014**, *22*, 7249.
- [273] A. A. Latiff, X. S. Cheng, M. F. M. Rusdi, M. C. Paul, S. W. Harun, H. Ahmad, *J. Nonlinear Opt. Phys. Mater.* **2018**, *27*, 1850010.
- [274] Z. K. Jiang, H. Chen, J. R. Li, J. D. Yin, *Appl. Phys. Express* **2017**, *10*, 122702.
- [275] J. T. Wang, W. Lu, J. R. Li, H. Chen, Z. K. Jiang, J. Z. Wang, W. F. Zhang, M. Zhang, L. L. Li, Z. H. Xu, W. J. Liu, P. G. Yan, *IEEE J. Sel. Top. Quantum Electron.* **2018**, *24*, 1.
- [276] W. J. Liu, M. L. Liu, J. D. Yin, H. Chen, W. Lu, S. B. Fang, H. Teng, M. Lei, P. G. Yan, Z. Y. Wei, *Nanoscale* **2018**, *10*, 7971.
- [277] J. T. Wang, W. Lu, J. R. Li, H. Chen, Z. K. Jiang, J. Z. Wang, W. F. Zhang, M. Zhang, I. L. Li, Z. H. Xu, W. J. Liu, P. G. Yan, *IEEE J. Sel. Top. Quant.* **2018**, *24*, 1100706.
- [278] D. Mao, X. Y. She, B. B. Du, D. X. Yang, W. D. Zhang, K. Song, X. Q. Cui, B. Q. Jiang, T. Peng, J. L. Zhao, *Sci. Rep.* **2016**, *6*, 23583.
- [279] J. Koo, J. Park, J. Lee, Y. M. Jhon, J. H. Lee, *Opt. Express* **2016**, *24*, 10575.
- [280] Z. Q. Luo, Y. Y. Li, M. Zhong, Y. Z. Huang, X. J. Wan, J. Peng, J. Weng, *Photonics Res.* **2015**, *3*, A79.
- [281] J. Lee, J. Koo, J. Lee, Y. M. Jhon, J. H. Lee, *Opt. Mater. Express* **2017**, *7*, 2968.
- [282] M. M. Wu, X. Li, K. Wu, D. D. Wu, S. X. Dai, T. F. Xu, Q. H. Nie, *Opt. Fiber Technol.* **2019**, *47*, 152.
- [283] J. Koo, J. Lee, J. H. Lee, *Advanced Solid State Lasers*, Optical Society of America, MA, USA, **2016**.
- [284] W. J. Liu, M. L. Liu, Y. Y. Ouyang, H. R. Hou, M. Lei, Z. Y. Wei, *Nanotechnology* **2018**, *29*, 394002.
- [285] J. T. Wang, Z. K. Jiang, H. Chen, J. R. Li, J. D. Yin, J. Z. Wang, T. C. He, P. G. Yan, S. C. Ruan, *Opt. Lett.* **2017**, *42*, 5010.
- [286] W. B. Gao, L. Huang, J. L. Xu, Y. Q. Chen, C. H. Zhu, Z. H. Nie, Y. Li, X. F. Wang, Z. D. Xie, S. N. Zhu, J. Xu, X. G. Wan, C. Zhang, Y. B. Xu, Y. Shi, F. Q. Wang, *Appl. Phys. Lett.* **2018**, *112*, 171112.
- [287] J. Koo, Y. I. Jhon, J. Park, J. Lee, Y. M. Jhon, J. H. Lee, *Adv. Funct. Mater.* **2016**, *26*, 7454.
- [288] G. M. Wang, *Opt. Laser Technol.* **2017**, *96*, 307.
- [289] J. T. Wang, Z. K. Jiang, H. Chen, J. R. Li, J. D. Yin, J. Z. Wang, T. C. He, P. G. Yan, S. C. Ruan, *Photonics Res.* **2018**, *6*, 535.
- [290] D. Mao, B. B. Du, D. X. Yang, S. L. Zhang, Y. D. Wang, W. D. Zhang, X. Y. She, H. C. Cheng, H. B. Zeng, J. L. Zhao, *Small* **2016**, *12*, 1489.
- [291] J. T. Wang, H. Chen, Z. K. Jiang, J. D. Yin, J. Z. Wang, M. Zhang, T. C. He, J. Z. Li, P. G. Yan, S. C. Ruan, *Opt. Lett.* **2018**, *43*, 1998.
- [292] X. Zhu, S. Chen, M. Zhang, L. Chen, Q. Wu, J. Zhao, Q. Jiang, Z. Zheng, H. Zhang, *Photonics Res.* **2018**, *6*, C44.
- [293] F. F. Lu, *Mod. Phys. Lett. B* **2017**, *31*, 1750206.
- [294] D. Steinberg, J. D. Zapata, E. A. T. Souza, L. A. M. Saito, *Conf. on Lasers and Electro-Optics (CLEO)*, IEEE, Piscataway, NJ, USA **2018**, https://doi.org/10.1364/CLEO_SI.2018.SM2N.3.
- [295] X. Xu, M. M. He, C. J. Quan, R. D. Wang, C. J. Liu, Q. Y. Zhao, Y. X. Zhou, J. T. Bai, X. L. Xu, *J. Lightwave Technol.* **2018**, *36*, 5130.

- [296] D. Mao, X. Q. Cui, X. T. Gan, M. K. Li, W. D. Zhang, H. Lu, J. L. Zhao, *IEEE J. Sel. Top. Quantum Electron.* **2018**, *24*, 1100406.
- [297] J. D. Yin, F. X. Zhu, J. T. Lai, H. Chen, M. Y. Zhang, J. Q. Zhang, J. T. Wang, T. C. He, B. Zhang, J. P. Yuan, P. G. Yan, S. C. Ruan, *Adv. Opt. Mater.* **2019**, *7*, 1801303.
- [298] Y. H. Shi, H. Long, S. X. Liu, Y. H. Tsang, Q. Wen, *J. Mater. Chem. C* **2018**, *6*, 12638.
- [299] J. Li, Y. F. Zhao, Q. Y. Chen, K. D. Niu, R. Y. Sun, H. N. Zhang, *IEEE Photonics J.* **2017**, *9*, 1.
- [300] K. D. Niu, R. Y. Sun, Q. Y. Chen, B. Y. Man, H. N. Zhang, *Photonics Res.* **2018**, *6*, 72.
- [301] H. R. Yang, X. M. Liu, *Appl. Phys. Lett.* **2017**, *110*, 171106.
- [302] J. J. Li, S. S. Zhang, Z. D. Bai, Z. W. Jia, Z. S. Man, S. G. Fu, *Opt. Eng.* **2018**, *57*, 096106.
- [303] M. Zhang, G. H. Hu, G. Q. Hu, R. C. T. Howe, L. Chen, Z. Zheng, T. Hasan, *Sci. Rep.* **2015**, *5*, 17482.
- [304] J. L. Wang, S. Li, Y. P. Xing, L. Chen, Z. Y. Wei, Y. G. Wang, *J. Opt.* **2017**, *19*, 095506.
- [305] K. Y. Lau, A. A. Latif, M. H. A. Bakar, F. D. Muhammad, M. F. Omar, M. A. Mahdi, *Appl. Phys. B* **2017**, *123*, 221.
- [306] J. Lin, K. Yan, Y. Zhou, L. X. Xu, C. Gu, Q. W. Zhan, *Appl. Phys. Lett.* **2015**, *107*, 191108.
- [307] H. Chen, Y. S. Chen, J. D. Yin, X. J. Zhang, T. Guo, P. G. Yan, *Opt. Express* **2016**, *24*, 16287.
- [308] L. Li, Y. G. Wang, Z. F. Wang, X. Wang, G. W. Yang, *Opt. Commun.* **2018**, *406*, 80.
- [309] B. H. Chen, X. Y. Zhang, K. Wu, H. Wang, J. Wang, J. P. Chen, *Opt. Express* **2015**, *23*, 26723.
- [310] H. Ahmad, M. A. Ismail, M. Suthaskumar, Z. C. Tiu, S. W. Harun, M. Z. Zulkifli, S. Samikannu, S. Sivaraj, *Laser Phys. Lett.* **2016**, *13*, 035103.
- [311] M. H. M. Ahmed, A. H. H. Al-Masoodi, A. A. Latiff, H. Arof, S. W. Harun, *Indian J. Phys.* **2017**, *91*, 1259.
- [312] H. D. Xia, H. P. Li, C. Y. Lan, C. Li, J. B. Du, S. J. Zhang, Y. Liu, *Photonics Res.* **2015**, *3*, A92.
- [313] J. H. Chen, G. Q. Deng, S. C. Yan, C. Li, K. Xi, F. Xu, Y. Q. Lu, *Opt. Lett.* **2015**, *40*, 3576.
- [314] R. I. Woodward, E. J. R. Kelleher, R. C. T. Howe, G. Hu, F. Torrisi, T. Hasan, S. V. Popov, J. R. Taylor, *Opt. Express* **2014**, *22*, 31113.
- [315] C. C. M. Martinez, A. Ambrosi, A. Y. S. Eng, Z. Sofer, M. Pumera, *Electrochem. Commun.* **2015**, *56*, 24.
- [316] H. Ahmad, H. Hassan, R. Safaei, K. Thambiratnam, M. F. Ismail, I. S. Amiri, *Opt. Commun.* **2017**, *400*, 55.
- [317] Z. Q. Luo, Y. Z. Huang, M. Zhong, Y. Y. Li, J. Y. Wu, B. Xu, H. Y. Xu, Z. P. Cai, J. Peng, J. Weng, *J. Lightwave Technol.* **2014**, *32*, 4679.
- [318] W. J. Liu, M. L. Liu, H. N. Han, S. B. Fang, H. Teng, M. Lei, Z. Y. Wei, *Photonics Res.* **2018**, *6*, C15.
- [319] C. S. Guo, B. H. Chen, H. Wang, X. Y. Zhang, J. Wang, K. Wu, J. P. Chen, *IEEE Photonics J.* **2016**, *8*, 1.
- [320] B. H. Chen, X. Y. Zhang, C. S. Guo, K. Wu, J. P. Chen, J. Wang, *Opt. Eng.* **2016**, *55*, 081306.
- [321] W. Y. Li, Y. Y. Ouyang, G. L. Ma, M. L. Liu, W. J. Liu, *Laser Phys.* **2018**, *28*, 055104.
- [322] H. Ahmad, M. A. Ismail, S. Sathiyam, S. A. Reduan, N. E. Ruslan, C. S. J. Lee, M. Z. Zulkifli, K. Thambiratnam, M. F. Ismail, S. W. Harun, *Opt. Commun.* **2017**, *382*, 93.
- [323] H. Ahmad, F. A. A. Rashid, S. R. Azzuhri, M. A. M. Salim, R. A. Shaharuddin, M. A. Ismail, M. Z. A. Razak, *Laser Phys. Lett.* **2016**, *13*, 115102.
- [324] H. Ahmad, M. Suthaskumar, Z. C. Tiu, A. Zarei, S. W. Harun, *Opt. Laser Technol.* **2016**, *79*, 20.
- [325] S. Ko, J. Lee, J. H. Lee, *Chin. Opt. Lett.* **2018**, *16*, 020017.
- [326] M. L. Liu, Y. Y. Ouyang, H. R. Hou, W. J. Liu, Z. Y. Wei, *Chin. Opt. Lett.* **2019**, *17*, 020006.
- [327] M. L. Liu, W. J. Liu, P. G. Yan, S. B. Fang, H. Teng, Z. Y. Wei, *Chin. Opt. Lett.* **2018**, *16*, 020007.
- [328] W. J. Liu, M. L. Liu, M. Lei, S. B. Fang, Z. Y. Wei, *IEEE J. Sel. Top. Quantum Electron.* **2018**, *24*, 1.
- [329] R. Y. Sun, H. N. Zhan, N. N. Xu, *Laser Phys.* **2018**, *28*, 085105.
- [330] K. D. Niu, Q. Y. Chen, R. Y. Sun, B. Y. Man, H. N. Zhang, *Opt. Mater. Express* **2017**, *7*, 3934.
- [331] X. Xu, M. Jiang, D. Li, R. D. Wang, Z. Y. Ren, J. T. Bai, *Opt. Quantum Electron.* **2018**, *50*, 39.
- [332] L. Li, R. D. Lv, J. Wang, Z. D. Chen, H. Z. Wang, S. C. Liu, W. Ren, W. J. Liu, Y. G. Wang, *Nanomaterials* **2019**, *9*, 315.
- [333] Y. H. Shi, W. J. Li, W. Lü, Q. Wen, in *2018 Asia Communications and Photonics Conf. (ACP)*, IEEE, Piscataway, NJ, USA **2018**, <https://doi.org/10.1109/ACP.2018.8596095>.
- [334] L. Du, G. B. Jiang, L. L. Miao, B. Huang, J. Yi, C. J. Zhao, S. C. Wen, *Opt. Mater. Express* **2018**, *8*, 926.
- [335] S. X. Wang, H. H. Yu, H. J. Zhang, A. Z. Wang, M. W. Zhao, Y. X. Chen, L. M. Mei, J. Y. Wang, *Adv. Mater.* **2014**, *26*, 3538.
- [336] A. Rodin, A. Carvalho, A. C. Neto, *Phys. Rev. Lett.* **2014**, *112*, 176801.
- [337] C. Han, M. Yao, X. Bai, L. Miao, F. F. Zhu, D. D. Guan, S. Wang, C. L. Gao, C. H. Liu, D. Qian, Y. Liu, J. F. Jia, *Phys. Rev. B* **2014**, *90*, 085101.
- [338] J. Kang, L. Zhang, S. H. Wei, *J. Phys. Chem. Lett.* **2016**, *7*, 597.
- [339] R. S. Chen, C. C. Tang, W. C. Shen, Y. S. Huang, *Nanotechnology* **2014**, *25*, 415706.
- [340] K. G. Zhou, M. Zhao, M. J. Chang, Q. Wang, X. Z. Wu, Y. L. Song, H. L. Zhang, *Small* **2015**, *11*, 694.
- [341] X. Huang, Z. Y. Zeng, H. Zhang, *Chem. Soc. Rev.* **2013**, *42*, 1934.
- [342] J. Jeon, J. Lee, J. H. Lee, *J. Opt. Soc. Am. B* **2015**, *32*, 31.
- [343] W. J. Liu, M. L. Liu, X. T. Wang, T. Shen, G. Q. Chang, M. Lei, H. X. Deng, Z. M. Wei, Z. Y. Wei, *ACS Appl. Nano Mater.* **2019**, *2*, 2697.
- [344] H. R. Mu, Z. T. Wang, J. Yuan, S. Xiao, C. Y. Chen, Y. Chen, Y. Chen, J. C. Song, Y. S. Wang, Y. Z. Xue, H. Zhang, Q. L. Bao, *ACS Photonics* **2015**, *2*, 832.
- [345] Z. T. Wang, H. R. Mu, C. J. Zhao, Q. L. Bao, H. Zhang, *Opt. Eng.* **2016**, *55*, 081314.
- [346] Z. T. Wang, H. R. Mu, J. Yuan, C. J. Zhao, Q. L. Bao, H. Zhang, *IEEE J. Sel. Top. Quantum Electron.* **2016**, *23*, 195.
- [347] Y. Q. Jiang, L. L. Miao, G. B. Jiang, Y. Chen, X. Qi, X. F. Jiang, H. Zhang, S. C. Wen, *Sci. Rep.* **2015**, *5*, 16372.
- [348] C. Liu, H. P. Li, G. L. Deng, C. Y. Lan, C. Li, Y. Liu, in *2016 Asia Communications and Photonics Conf. (ACP)*, OSA Publishing, USA **2016**, <https://doi.org/10.1364/ACPC.2016.AF2A.129>.
- [349] W. X. Du, H. P. Li, C. Liu, S. N. Shen, C. Y. Lan, C. Li, Y. Liu, *Proc. SPIE* **2017**, *10457*, 104571M.
- [350] S. X. Liu, Z. J. Li, Y. Q. Ge, H. D. Wang, R. Yue, X. T. Jiang, J. Q. Li, Q. Wen, H. Zhang, *Photonics Res.* **2017**, *5*, 662.
- [351] H. Chen, J. D. Yin, J. W. Yang, X. J. Zhang, M. L. Liu, Z. K. Jiang, J. Z. Wang, Z. P. Sun, T. Guo, W. J. Liu, P. G. Yan, *Opt. Lett.* **2017**, *42*, 4279.
- [352] W. J. Liu, M. L. Liu, B. Liu, R. G. Quhe, M. Lei, S. B. Fang, H. Teng, Z. Y. Wei, *Opt. Express* **2019**, *27*, 6689.
- [353] Q. L. Bao, K. P. Loh, *ACS Nano* **2012**, *6*, 3677.
- [354] A. Martinez, Z. P. Sun, *Nat. Photonics* **2013**, *7*, 842.
- [355] X. P. Hong, J. Kim, S. F. Shi, Y. Zhang, C. H. Jin, Y. H. Sun, S. Tongay, J. Q. Wu, Y. F. Zhang, F. Wang, *Nat. Nanotechnol.* **2014**, *9*, 682.
- [356] Y. F. Yu, S. Hu, L. Q. Su, L. J. Huang, Y. Liu, Z. H. Jin, A. A. Purezky, D. B. Geohegan, K. W. Kim, Y. Zhang, L. Y. Cao, *Nano Lett.* **2015**, *15*, 486.